LUNDS UNIVERSITET

Lunds Tekniska Högskola

Study of tomato fiber fragmentation in the high-pressure homogenizer

Maytham Alameri

Master of Science Thesis 2018

Department of Food Technology, Engineering and Nutrition Food

Lund University

Study of tomato fibers fragmentation in the high-pressure homogenizer

Master thesis by:

Maytham Alameri

Department of Food Technology, Engineering and Nutrition,
Lund Institute of Technology, Lund University, Sweden
In cooperation with Tetra Pak Processing Components AB

Master of Science Thesis 2018

Academic supervisor: Assoc. Prof. Andreas Håkansson, Department of Food Technology, Engineering and Nutrition

Industrial supervisor: Prof. Fredrik Innings, Tetra Pak Processing Components AB, Lund

Examiner: Prof. Björn Bergenståhl, Department of Food Technology, Engineering and Nutrition

AKNOWLEDGEMENTS

Firstly, I would like to acknowledgment my thesis supervisors Assoc. Prof. Andreas Håkansson of the Food Technology department at Lund University and Prof. Fredrik Innings from Tetra Pak, for all the help, the motivation and support they have been given during the thesis work. I would like to thank you both for encouraging my research and for guiding me in all the time of study and writing of this thesis. Their advice on both research as well as on my career have been invaluable. I could not have imagined having better advisors and mentors for my thesis work.

Furthermore, special thanks for Jozo Valencuk from Tetra Pak for his help to set up and maintain the high-pressure homogenizer in good condition for this thesis work.

I am also grateful to Dan Johansson, Hans Bolinsson and other colleagues in Kemicentrum, Lund University for their unfailing support and assistance about the equipment and measuring methods related to this project.

I would also like to express my appreciation to Professor Björn Bergenståhl of the Food Technology department at Lund University as my examiner of this thesis, and I am gratefully indebted to her for her valuable comments on this thesis.

Finally, a special thanks to my family words cannot express how grateful I am to my wife, my mother, my father, aunt and my father in law. For all the sacrifices that have been made. For the encouragement and love to help me make through the project. They are the most important people in my world, and I dedicate this thesis to them.

Abstract

Homogenization is commonly used in many food processes in which products pass through a narrow gap causing break down of large particles into smaller one thereby reducing creaming and sedimentation of the products.

This study aims to investigate fragmentation of tomato fibers and test which breaking mechanisms are dominating in a high-pressure homogenizer. The study also includes the influence of several passages' homogenization.

Numerous mechanisms of particles disruption have been proposed, including viscous shear, turbulence, cavitation, squeezing and impingement with a solid surface. However recent researches suggested fragmentation by turbulence, and cavitation as the primary mechanisms for emulsions drop break up in the homogenization valve. The study discusses fragmentation by laminar shear, turbulent inertial, turbulent viscous as well as squeezing.

Several hypotheses have been suggested to explain which breaking mechanisms are controlling fiber fragmentation in the high-pressure homogenizer. Each of the mechanism results in quantifiable predictions about operating conditions: The laminar viscous mechanism implies that increasing of homogenization pressure and continuous phase viscosity would lead to smaller particles size for the tomato suspension. Turbulent inertial implies no impact of serum viscosity on the particles break up, while turbulent viscous predict that higher continues phase viscosity results in smaller particles size. Both of turbulent theories agreed on smaller suspension particles obtained by higher homogenization pressure with a relation described as $d_{max} \propto \Delta P^{-1}$ in turbulent viscous regime and $d_{max} \propto \Delta P^{-4/5}$ in turbulent inertial system. For the fiber squeezing by the homogenization gap, it is expected that smaller gap height will result in smaller fiber particles of the tomato suspension. Experiments were carried out to investigate if these trends could be seen in data, and thus if any of the suggested mechanisms could be rejected.

The results revealed that high homogenization pressure increases the homogenization efficiency and smaller particles size obtained. However, the calculated slope from laser diffraction results was -0.599 for the 18.8% of tomato concentrate juice and -0.523 for the juice of 9.2% of tomato concentrate which not match the expected value of the laminar shear, turbulent inertial and turbulent viscous. The influence of the serum viscosity on the particles size showed higher serum viscosity result in larger particles size. Most significant reduction of size was obtained by the lowest continues phase viscosity which disapproves the influence of the most often suggested mechanisms. The result obtained by different gap height shows no apparent effect of the gap height on the size of tomato fiber, such a result explains that squeezing plays no role in fiber fragmentation. Moreover, the size distribution results were confirmed by microscope images and rheology measurements. Several passages showed the capability of tomato fiber to break up even after 32-time homogenization and particles would continue to fragment with further homogenization.

In conclusion, this study has shown that most previously suggested mechanisms do not correspond with tomato fiber breakup and further investigations are needed.

Abbreviation

Symbol	Description	Unit
HPH	High pressure homogenizer	
d_{43}	Volume base average particle size	µm
d_{32}	Surface base average particle size	µm
Q	Flow rate	Lh^{-1}
r_i	Gap inlet raduis	m
r_e	Gap exit radius	m
Re	Reynolds number	
u	Local fluid velocity	ms^{-1}
ρ	Mass density of the liquid	kgm^{-3}
v	kinematic viscosity of the liquid	m^2s^{-1}
L	The characteristic length	m
h	Gap height	m
U_g	Gap velocity	ms^{-1}
ρ_c	Mass density of the continuous phase	kgm^{-3}
η_c	Dynamic viscosity of the continuous phase	Pas
p	Dynamic pressure	Pa
γ	Surface tension	Nm^{-1}
We	Weber number	
Ca	Capillary number	
G	Velocity gradient	s^{-1}
d	Drop diameter	m
We_{cr}	Critical Weber number	
τ_{def}	Drop deformation timescale	s
d_{max}	Maximum drop size	m
σ_{frag}	Fragmentation Stress acting on the drop	Pa
$\bar{u}$	Time average of velocity	ms^{-1}
u’	root mean square average of velocity	ms^{-1}
ε	Energy dissipation rate per unit mass	m^2s^{-3}
λ	Kolmogorov length scale	m
$\bar{\varepsilon}$	Mean value of dissipation rate per unit mass	m^2s^{-3}
l_e	Eddy length in intertrial region	m
l	Eddy length scale	m
N_c	Cavitation number	
d_j	Orifical diameter or jet diameter	m
X	Distance between the gap and impingement ring	m
PSD	Particle size distribution	
n_i	Percentage of particles	
NH	Number of passages	
Re_i	Inlet-radius based Reynolds number	
Δp_{IC}	Homogenizing pressure in the inlet chamber	Pa
Δp_{gap}	Homogenizing pressure in the gap	Pa
Δp_{OC}	Homogenizing pressure in the outlet	Pa

Table of Contents

1 Context and background

1.1 Introduction

High-pressure homogenization (HPH) is a technology that is widely used in different types of application such as food, chemical and pharmaceutical industry. The most common food application is probably the homogenization of milk, which serves to reduce the size of the fat globule, thus reducing the rate of creaming and sedimentation. Roughly, 270 Mt of dairy products are processed with high-pressure homogenization annually (IDF, 2010). The importance of the homogenizer in the dairy process and other industry sectors encourage the world to investigate the fundamental part of drops and particles fragmentation, and establish several theories explaining which mechanisms control fragmentation. Furthermore, understanding the fragmentation process benefits on the efficiency and application of the homogenization process, as well as the design of the homogenization valves.

The tomato industry is one of the most advanced, globalized and innovative horticultural sectors, furthermore, tomato is considered as one of the most important vegetables in the food industry. The world production of fresh and processed tomatoes was estimated to be 170 million tons in 2014 according to the Food and Agriculture Organization FAO (FAO ,2007). However, approximately 80% of tomatoes consumption are in the form of processed tomato products, which make tomatoes the world's leading vegetable for processing (Lehkoživová et al., 2009). Homogenization is a common unit operation in the production of tomato products. Homogenization affects the rheology properties of tomato products by reducing the particle size of tomato suspension. Previous studies of rheology properties of homogenized tomato products indicated an increase in the consistency and improvement of sensory acceptance of the tomato products (Kubo et al., 2013). Therefore, this study of how tomato fibers break up as well as breaking mechanisms are essential for an efficient product and process design.

1.2 An historical perspective of the homogenizer

In the 1890s, the French engineer Auguste Gaulin invented the first model of the homogenization device (Francis, 1999). The machine was patented in 1899 by Gaulin with the purpose of fixing, stabilizing a fat emulsion against creaming and gravity separation. Gaulin presented the device to the world for the first time at the world fair in Paris 1900 (Francis, 1999; Innings, 2015). In 1901, Gaulin manufactured his first homogenizer by Manton-Gaulin Manufacturing Company. During the period from 1900 to 1930s, the design of the device changed several times and led to the innovation of the two-stage homogenizer by Gaulin in 1925.

Throughout the years the usage of high-pressure homogenizer increased, and it was used all over the world for different applications such as, chemicals, pharmaceutical and biotechnology industry.

From the beginning of the homogenization process different theories were established trying to explain the fundamental part of the drop breakup. Gaulin speculated that mechanical interaction between the gap wall and the drops leads to the fragmentation of the drops (Gaulin, 1904). However, this explanation was soon disproved when it became clear that the machine has a large gap size comparing to the size of the initial drop size (Håkansson, 2015).

Another suggestion proposed that fragmentation of the drops is a result of a collision of the drops with the impact ring in the outlet chamber. This occurs when the drop has high velocity enough to reach the impact ring (Håkansson, 2015). Innings observes that drop velocity decrease rapidity in the gap exit as a function of distance (Innings & Trägårdh, 2007). Analyzes of the jet images on exit chambers show that the drop cannot travel far without breaking up (Innings et al., 2011). Thus, impingement cannot be considered as a fragmentation mechanism. Then researchers searched for more reliable breaking theory explaining drops breakup in HPH.

1.2 The homogenizer

The homogenizer is a common unit operation used in the production of the tomato products. The technology is usually classified depending on homogenization pressure; The ultrahigh-pressure homogenization for homogenization pressure up to 350-400MPa, or a high-pressure homogenization when the pressure is between 150-200 MPa (Trujillo et al., 2016).

The high-pressure homogenizer consists of two major components: a high-pressure piston pump and a narrow gap. However, the tomato suspension enters the pump back and the piston pump pressurize fluid suspension, which force it to pass through the homogenization gap. In the gap, the pressure convened into velocity and the particles confront several forces leading to break up (Innings, 2005).

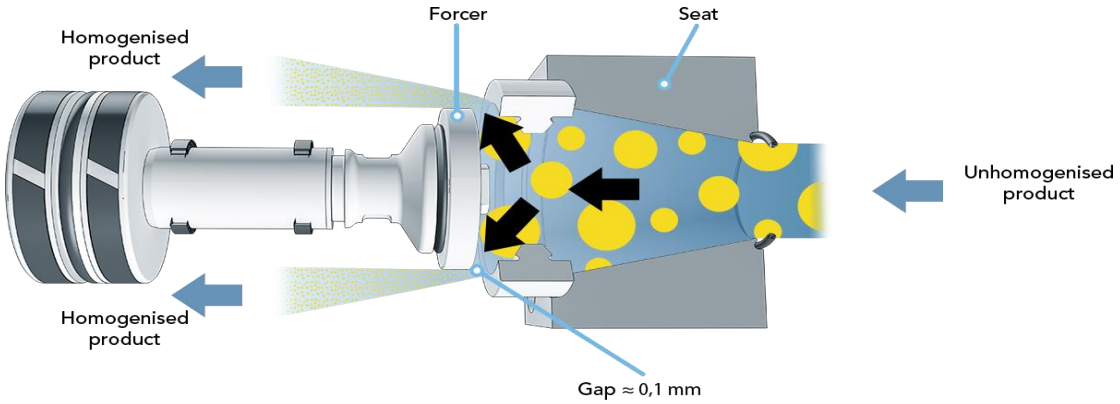

Figure 1: Illustration shows the working of the homogenization device (Bylund, 2015).

1.2.1 The high-pressure pump

A piston pump is a positive pump that creates a pressure of 10 to 500 MPa (Innings, 2005; Bylund, 2015). The capacity of the pump depends on the speed of the motor as well as the size of the piston. The pump of the homogenizer is designed to deliver a constant flow rate, with a range from a few liters per hour for the small-scale machine, up to 53000 liters per hour for the large production scale machine (Francis, 1999).

1.2.2 The homogenization device

A homogenizer can consist of one homogenization head referred to as single stage homogenizer, or It may consist of two homogenization heads in series, called a two-stage homogenizer. In the single stage homogenizer, the homogenization pressure (P1) applied over the first head, and the back pressure(P2) is generated by the process.

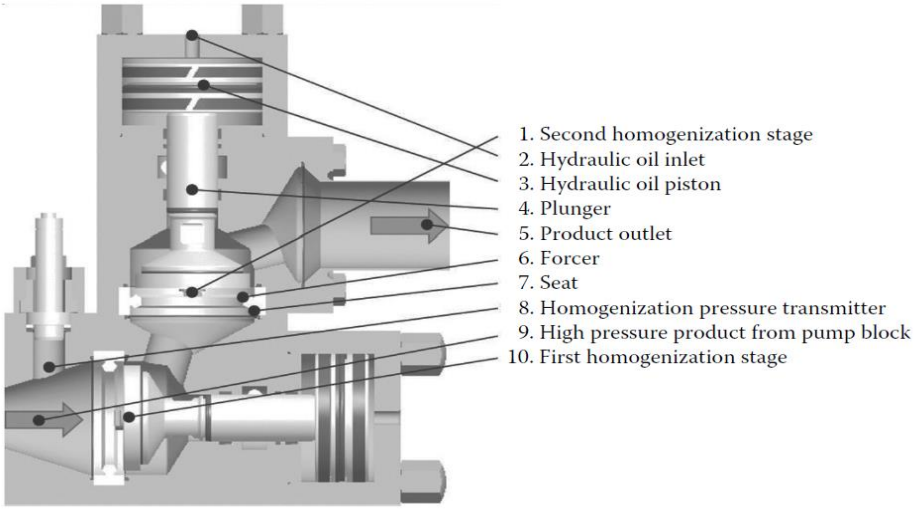

Figure 2: Detailed structure of the two-stage homogenization device (Innings, 2015).

In the two-stage homogenizer, the second homogenization head is creating the back pressure, which is usually used to maintain optimal homogenization efficiency. Two-stage homogenizers are commonly used in food application with second stage homogenization pressure around 20% of that in the first stage to obtain the best homogenization result (Bylund, 2015). A specified structure of the two-stage homogenizer is shown in Figure (2).

The product is a pump to the homogenization valve utilizing a positive-displacement pump. At the homogenization valve, the fluid velocity increases as it is pushed through the first-stage gap between the seat and the forcer, then the fluid accelerates again as it is forced through the second stage homogenization gap. Upstream of the gap, the seat gives rise to a narrow region known as the inlet chamber. The fluid exits as a jet to a large space downstream of the gap referred to as the outlet chamber. The outlet chamber is equipped with a unique impact ring to adjust the outlet chamber geometry (Håkansson, 2015).

The gap height is not fixed and can be adjusted by lowering and raising the position of the forcer by controlling the homogenization pressure — illustration for homogenization head shown in Figure (3).

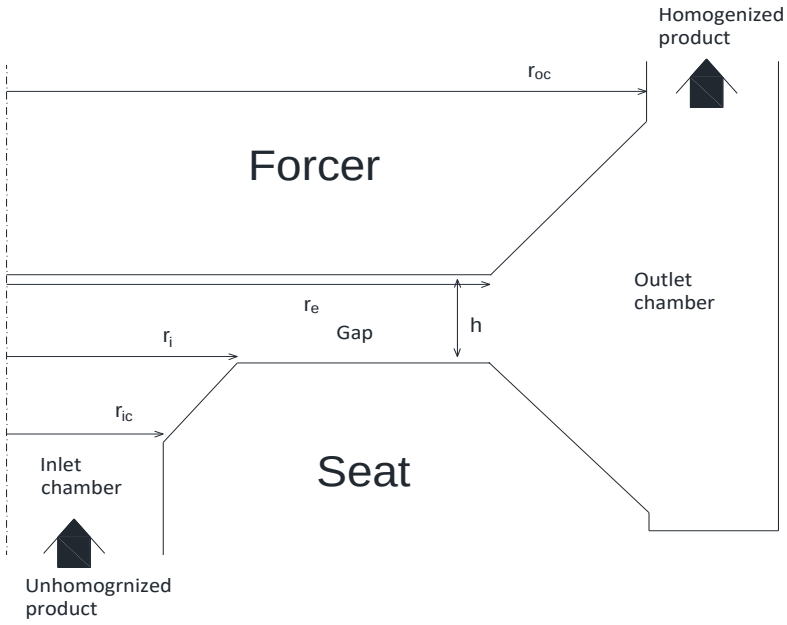

Figure 3: Illustration describes the homogenization valve (redrew using AutoCAD 2018 from Håkansson, 2017).

2 Objective and research questions

The major objective of the project is to increase the fundamental understanding of tomato fiber break in the high-pressure homogenizer by investigating which fragmentation mechanisms are consistent with experimentally observed trends with operating conditions.

To reach the objective the following questions will be answered:

1. How fiber breakup is affected by increasing the homogenization pressure?
2. Will increasing the continues phase viscosity of the product lead to bigger or smaller particles size of the homogenized products?
3. How fiber breakup is affected by gap height?
4. Will fiber continue to break up when homogenizing it for several passages?
5. How does rheological properties of the products change with homogenization pressure, gap height and several passages?

3 Theory

3.1 Fruit and tomato structure

During the homogenization process of a tomato product, mechanical force is applied to the tomato causing drastic changes in the physical properties, as well as the microstructure of the tomato product. Understanding the microstructure of tomato suspension before and after homogenization is necessary to also understand the mechanism in which these forces are affecting the tomato product or any other types of food with a similar composition.

There are two phases in the structure of the tomato juice: an insoluble phase (pulp or dispersed phase) in a viscous solution (serum or continues). The dispersed phase consists of tissue cells and their fragments, cell walls and insoluble polymers. The serum phase includes soluble polysaccharides, sugars, salts and acids (Augusto et al., 2012).

The main fraction of cells in tomato products is Parenchyma cells. These cells have an almost spherical shape and function mainly as general-purpose plant cells with a three-layer cell wall.

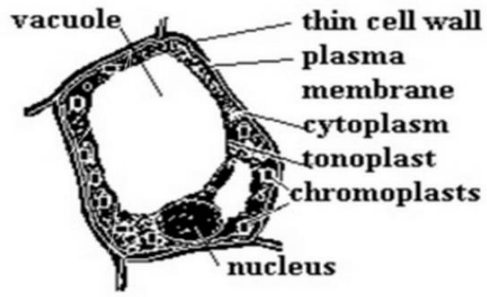

Figure 4: Parenchyma cell of tomato (Elfick, 2018).

Den Ouden and Van Vliet (1997) suggested that these cells are highly deformable and can pass through a pore of the sieve with a smaller size than its original size (Ouden & Vliet, 1997).

In Figure (5) the structure of a tomato cell wall is shown. The cell wall structure consists of three layers; primary, secondary cell wall, and middle lamella. The primary function of the cell wall is to support the cell structure, provide it with protection, maintain the shape and form of the cell as well as involve in transporting the material and metabolites into and out of the cell.

The primary cell wall is composed of the polysaccharides´ cellulose, hemicelluloses, and pectin. Cellulose is the main chemical component of the primary cell wall and exits in the form of microfibrils that composed of thousands of glucose molecules. Pectin and hemicelluloses are branched polysaccharides that organized in the form of a gel-like matrix that contains cellulose microfibrils.

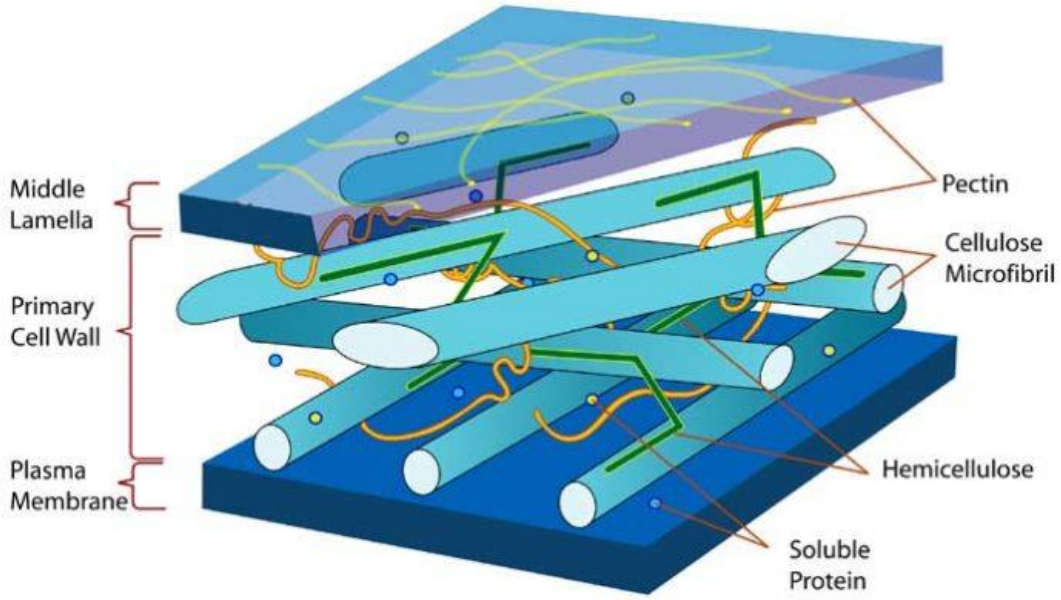

Figure 5: Cell wall structure of plant cell wall (Bailey, 2018).

The composition of the secondary cell wall includes cellulose, hemicelluloses, and rich in lignin. This rigid layer forms inside the primary cell wall when the primary cell wall stops to grow. Lignin confers support and mechanical strength to the secondary cell wall.

In additional plant cell walls include a small amount of proteins. A part of cell wall proteins contributes to the structure and the mechanical strength of the wall. The outer layer of the cell wall is known as a middle lamella, and it is composed mainly from pectin. The middle lamella functional as a binder for the neighboring cells which enables the cells to shear their content with each other. Pectin fragments in the middle lamella are contacted directly to the softening of the fruit tissues.

The highest concentration of pectin is in the pant tissue mainly located in the middle lamella of the cell wall. Pectin is soluble in hot water, except for the protopectin parts that usually found in unripe fruits. Thus, depending on the solubility of pectin two types of pectin are recognized: water-insoluble pectin and water-soluble pectin (Thakur et al., 1997).

One of the most critical capability for pectin is the ability to form a gel which is contributed to increasing the viscosity and consistency of fruit products — characteristics of pectin gel as in solubility is affected by molecular weight and DE. The

gel formation ability, solubility, and viscosity are usually related. For example, increase the viscosity due to increase the molecular weight will lead to increase in the tendency to form a gel as well as a decrease in the solubility of pectin (Sriamornsak, 2003).

Furthermore, the gel formation capacity is influenced by several factors such as pH, temperature, and the presence of counter ions or liquefied substances (Sriamornsak, 2003). For instance, in tomato process, higher breaking temperature is applied for the inactivation of enzymes result in a higher flow resistance due to the retention of pectin (Thakur et al., 1996).

Previous studies have reported that the presence of soluble pectin in the continuous phase contributes to an increase in the viscosity of the fruit suspension (Reo, 2010). Numerous studies have considered the viscosity of continuous and dispersed phases as an essential factor that affects the homogenization effectiveness (Innings, 2005; Kolb, 2001); thus, the concentration of pectin can be considered as an important factor in tomato juice homogenization.

3.2 Fruit juice definition

Fruit juice (Including tomato juice) was defined by Codex Alimentarius Commission of food stander supplied by FAO and WHO in General Standard for Fruit Juices and Nectars (CODEX STAN 247-2005) as the following:

"Fruit juice is the unfermented but fermentable liquid obtained from the edible part of sound, appropriately mature and fresh fruit or of fruit maintained in sound condition by suitable means including post-harvest surface treatments applied in accordance with the applicable provisions of the Codex Alimentarius Commission.

Some juices may be processed with pips, seeds and peel, which are not usually incorporated in the juice, but some parts or components of pips, seeds and peel, which cannot be removed by Good Manufacturing Practices (GMP) will be acceptable."

3.3 Tomato juice production

Tomato juice production begins with harvesting and transporting of tomato into a storage house at the production facility. The degree of ripeness at the harvesting time changes the utilization characteristic of tomatoes such as wholeness, serum viscosity and the percentage of soluble solids. (Leonard, 1971). Preparation of tomato for processing start with washing the tomatoes with water using either sample static tanks or high-pressure water jets (Goose & Binsted, 1973). Afterward, sorting and trimming of tomato starts to avoid any defective materials.

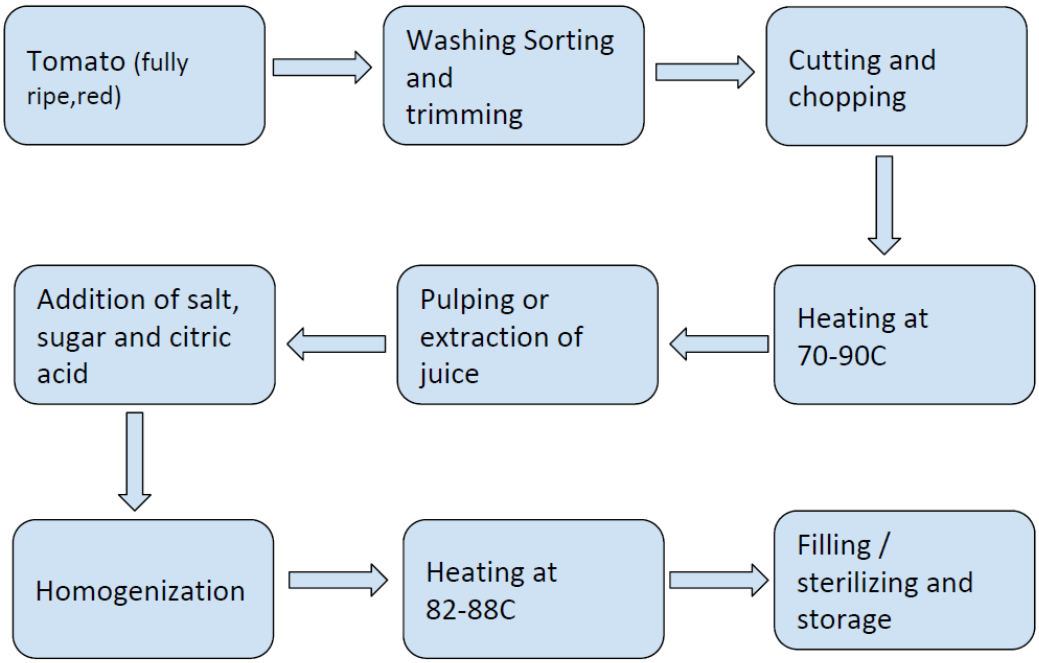

Figure 6: Production line of tomato juice.

Then, a starting of a combination of crushing, chopping, and slicing of tomato with different heat treatment to inactivation of the enzyme. The enzyme inactivation is known as a hot break when the treatment temperature more than 85˚C or a low temperature less than 70˚C then it is called as a cold break (Tornberg, 2016). The consistency of the final product is profoundly affected by the inactivation of pectin enzyme of fresh tomato. Several types of research reported that the breakdown of pectin material by enzymatic action results in a product with low viscosity. Thus, as expected that the cold break is resulting product with low consistency comparing to hot break due to pectin degradation by the action of a specific enzyme (Tornberg, 2016).

3.4 Homogenized juice

Microscopic examining of tomato suspension before the homogenization shows drastic changing of tomato suspension before and after homogenization process as is shown in Figure (7) (Bayod, 2008). The unhomogenized tomato suspension consists of large whole tomato cells, as well as other cellular materials. While, after homogenization, the juice forced to pass through a gap, which will damage and break up tomato cells result in a number of small size particles that are composed mainly form the cells materials as well as fragmentation of the cell wall materials (Lopez et al., 2011). As a result of altering size distribution, a fiber network is formed, which tends to hold a more significant amount of the continuous phase in the product (Panozzo et al., 2013).

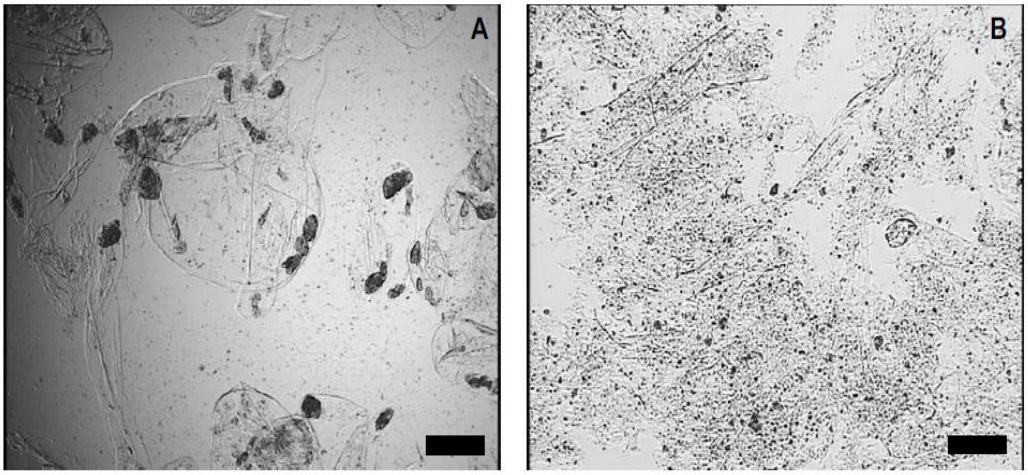

Figure 7: Microstructure of tomato suspension under microscope before and after homogenization. The scale bar is 150 µm (Bayod, 2008).

Furthermore, the surface area is increased resulting in higher interaction among the suspension particles (Augusto et al., 2012). More fiber aggregates are caused by small fiber particles and the high interaction between particles (Bengtsson et al., 2011). Thus, several studies have reported that homogenization alters the nature of the suspension network and improve the rheology properties of the suspension (Bayod, 2008).

3.5 Introduction to fluid dynamic of the homogenization

As was mentioned before, the homogenizer consists of a pump that forces the fluid to pass through a narrow gap where the fluid velocity is rapidly increased result in a different flow pattern within the homogenizer. The two types of flow, which can be distinguished in the homogenizer are a laminar or turbulent flow. The flow type depends on the fluid position in HPH. The flow is laminar as the flow tends to be a sheet-like in which the fluid drops move in parallel layers. In turbulent flow, the fluid undergoes an irregular movement of particles in which the fluid speed at a point is continuously changing in both magnitude and direction due to this movement the flow can counter eddies that intersect the overall movement of the fluid.

The primary method to characterize the flow pattern whether a laminar or turbulent flow is by using Reynolds number (Re):

$$\mathrm{Re} = \frac{\mathrm{u}L\rho}{\eta} \qquad \text{(Eq.1)}$$

Reynolds number inside the gap can be found from equation (2) (Phipps, 1975):

$$\mathrm{Re} = \frac{Q\rho}{2\pi r_e \eta} \quad \text{(Eq.2)}$$

There are two types of disruptive forces that lead to drops fragmentation in HPH: a frictional (i.e., viscous or shear force) and an inertial force. Viscous forces, by definition, are dominant in the regions of the laminar flow, and the breakup regime designates as a laminar viscous (LV). In turbulent flow, the breakup regimes are defined as a turbulent inertial (TI), or viscous forces cause the particles fragmentation then the regime is known as a turbulent viscous (TV).

The valve unit geometry governs the flow characteristics of the fluid. However, the displacement piston pump of the homogenizer is designed to deliver an almost constant flow rate. The flow rate of the gap can be obtained by using equation (3) (Håkansson, 2017):

$$Q = 2\pi r_e h U_g \quad \text{(Eq.3)}$$

Since the gap height is not fixed (depends on the forcer position), a higher homogenization pressure is required to maintain the same flow rate to overcome fractional flow forces for small gap height.

The total pressure drop in the valve gap is set by regulating the force applied on the forcer, which in turn, adjusted the gap height and usually given by using correlations such as (Phipps, 1975):

$$\begin{aligned} \Delta p &= \Delta p_{IC} + \Delta p_{gap} + \Delta p_{OC} \\ &= \frac{1}{4}\left[\frac{Q}{2\pi r_i h}\right]^2 + \Delta p_{gap} + \frac{1}{2}\left[\frac{Q}{2\pi r_e h}\right]^2 \end{aligned} \quad \text{(Eq.4)}$$

Since most of the pressure loss occurs at the exit chamber of the homogenizer, the homogenization pressure can be expressed by the third terms of equation (3), and the homogenization pressure can obtain as following (Håkansson, 2015):

$$\Delta p = \frac{\rho_c {U_g}^2}{2} \quad \text{(Eq.5)}$$

3.6 Fragmentation theory of emulsion droplets

When explaining and discussing the breaking mechanisms, it is important to mention that the different mechanisms are set to explain emulsions break up in the homogenization valve, and they have been tested on tomato suspension in this diploma work. This section discusses emulsion breakup theory. A discussion on cell breakup can be found in Section 3.7.

The most common fragmentation theories proposed for emulsions droplets are fragmentation by laminar shear, turbulence, and cavitation (Håkansson, 2015). The breakup is a result of external forces which is act via the continuous phase (Walstra & Smulders, 1998).

Most of the fragmentation mechanisms are based on the relation between the disruptive forces (pulling drops apart) to the interfacial forces (holding the drop spherical). This relation is known as a capillary number (Ca) when the disruptive forces are based on viscose forces, or a Weber number (We) when the disturbing force are based on the inertial forces (Innings,2005).

$$We = \frac{\text{inertial force}}{\text{interfacial tension force}} = \frac{\rho_c U^2}{4\gamma} \qquad \text{(Eq.6)}$$

$$Ca = We_L = \frac{\text{viscous force}}{\text{interfacial tension force}} = \frac{\eta_c G d}{2\gamma} \qquad \text{(Eq.7)}$$

The most critical factor, which affects the particles break up, is homogenization pressure. With an increase in the homogenization pressure, smaller mean particle size was obtained for homogenized milk (Walstra et al., 1998, kolb et al., 2001).
Several studies suggested the continuous phase viscosity as an essential factor that affects the homogenization efficiency, and an increase in the serum viscosity will lead to a smaller emulsions' droplets (Walstra, 1983).

3.6.1 Laminar Shear (LV)

Here fragmentation of drops is a result of the viscous forces that generate by the velocity gradient inside the viscous product. In general, the LV regime occurs when Re flow <1000 and Re drop <1 (Walstra & Smulders, 1998). The two possible scenarios that occur in laminar shear are simple shear and purely elongational, see Figures (8). In the simple shear, the particles start to rotate due to higher liquid velocity in the top of the particles comparing to the velocity in the bottom of particles, or the liquid itself inside the particles start to rotate. While purely elongational causes particles elongation and deformation due to viscous drag on the interface (Rayner, 2015; Håkansson, 2015).

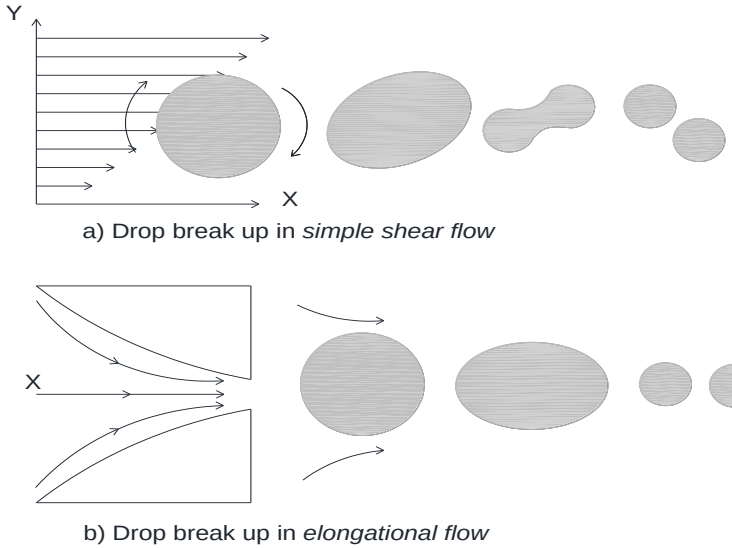

Figure 8: Illustration shows drops deformation and fragmentation in laminar flow under: Simple shear flow (a) and elongational flow (Redrew using AutoCAD 2018 from Rayner, 2015).

The Fragmentation stress applied on the drops described as function of velocity gradient as shown (Walstra & Smulders, 1998):

$$\sigma_{frag} = \eta_c G \qquad \text{(Eq.8)}$$

The deformation of the drops is described by the ratio between viscous forces and Laplace pressure, i.e. Weber number (We), equation (6). The drops break up into smaller drops when the drops are long enough to divide into smaller ones that occur approximately as the drops twice long as thin drops (Håkansson, 2015). Based on Equations (6 & 7), the deformation of the drops increases by increase Weber number until it reaches above a critical value (We_{cr}) that leads to the drops burst (Walstra & Smulders, 1998).

Several studies have suggested that fragmentation of drops depends on the viscosity ratio of the fluid (ratio of dispersed phase viscosity to continuous phase viscosity) which affects the critical Weber number required for the drops break up. For the simple shear maximum droplet size are expressed by Equation (9) (Walstra & Smulders, 1998; Walstra, 1993).

$$d_{max} = \frac{2\gamma We_{cr}}{\eta_c G} \qquad \text{(Eq.9)}$$

From equation (8) and (9), it is possible to conclude that increases of the continues phase viscosity will lead to increase in the fragmentation force applied on the drops result in smaller particles size.

Furthermore, previous research has indicated that if the viscosity of the dispersed has four times more than the viscosity of continuous phase, the drop begins to rotate without breaks up in a simple shear (Walstra,1983). Thus, Walstra argued that the only drop with low viscosity has the necessary time to deform.

Håkansson observed that the high laminar shear exists in two locations in the homogenization valve: at the inlet chamber, and the boundary layers of the gap (Håkansson et al., 2011). In the inlet chamber, the laminar shear was a result of increase fluid speed as it was passing through a smaller area before entering the gap (Håkansson,2015). Flow profile of the drops in the gap showed that the vast majority of the drops pass through the center of the gap. Thus, it is expected that the boundary layers would not have a significant effect on the result of the homogenization (Håkansson,2015).

3.6.2 Fragmentation by turbulence

The fluid speed accelerated as it was passing through the homogenization gap, due to high pressure applied to the product upstream of the homogenization valve. The rapid acceleration of the liquid in the narrow gap creates a jet flow downstream of the homogenization valve. The kinetic energy is stored in the jet give rise to the formation of coherent structures know as turbulent eddies. A portion of this turbulence dissipated as thermal energy, when the jet broke-up, otherwise it contributed to particles disruption (Innings, 2005; Håkansson et al., 2011).

Previous research has indicated that eddies with different length scale affecting particles differently which means that particles disruption in turbulent flow connects to length scales of these eddies, l. Thus, Kolmogorov theory used as scaling laws, Kolmogorov length scale can be calculated using (Håkansson, 2015):

$$\lambda = \left[\frac{\nu^3}{\varepsilon}\right]^{1/4} \qquad \text{(Eq.10)}$$

Where ε defines as the energy dissipation rate per unit mass. Eddies with different length scales have a various amount of turbulent, which will influence drops fragmentation differently. Innings has estimated the mean efficient value of dissipation rate as following (Innings & Trägårdh, 2007):

$$\bar{\varepsilon} = \frac{{U_g}^3}{80h} \quad \text{(Eq.11)}$$

Kolmogorov–Hinze discarded the drops fragmentation in turbulent flow in two primary mechanisms: a turbulent inertial (TI), and turbulent viscous (TV). An essential aspect of the Kolmogorov theory is to identify the dominating turbulent flow mechanisms and which length scale contributing more to drops breakup within the HPH.

Visualization of particles fragmentation has suggested that the particles fragmentation happens in the outlet chamber. Thus, Innings and Trägårdh identify the drops fragmentation in turbulent flow as a primary mechanism for drops break up in HPH (Innings & Trägårdh, 2005).

3.6.2.1 Turbulent inertial (TI)

Inertial fragmentation originates from the smallest length-scale eddies in the system, comparable in size or smaller than the droplets, i.e.$l < d$, an illustration of particles break up in turbulent inertial shown in Figure (9). In this case, the distribution of particles occurs due to pressure fluctuations act over the surface of the particles, however, the fragmentation stress acts over the drops can be calculated from (Håkansson,2015):

$$\sigma_{frag} = \frac{\rho_c u'}{2} \quad \text{(Eq.12)}$$

Eddies with large length scale have a higher degree of velocity fluctuations, u'. The kinetic energy of the large eddies transfers to small eddies which have smaller u'. Thus, small eddies have higher kinetic energy content and larger velocity gradient (u'/l).

Walstra has suggested a relationship between the maximum size of drops can survive without breakup in TI regime and energy dissipation of the eddies (Walstra & Smulders,1998) as shown:

$$d_{max} \approx \varepsilon^{-2/5} \gamma^{3/5} \rho_c^{-1/5} \quad \text{(Eq.13)}$$

The above equation shows that higher dissipation rate will lead to smaller particles size and changing of the continuous phase viscosity will not influence the maximum size of drops resulting in this regime.

3.6.2.2 Turbulent viscose (TV)

The drop Fragmentation in this regime is due to viscous forces created by eddies of a length scale much larger than the drops, as shown in Figure (9). Since the acting force is

similar to laminar viscose, then shear forces acts on the surface of the drops are changing with continuous phase can be found from:

$$\sigma_{frag} = \eta_c \frac{u'}{d} \quad \text{(Eq.14)}$$

Moreover, the maximum drop size survived the breakup is given by:

$$d_{max} = \gamma \varepsilon^{-1/2} \eta_c^{-1/2} \quad \text{(Eq.15)}$$

The above equation (15) shows that fragmentation of drops in TV regime depends on the continuous phase viscosity and a higher continuous phase viscosity will lead to smaller particles size.

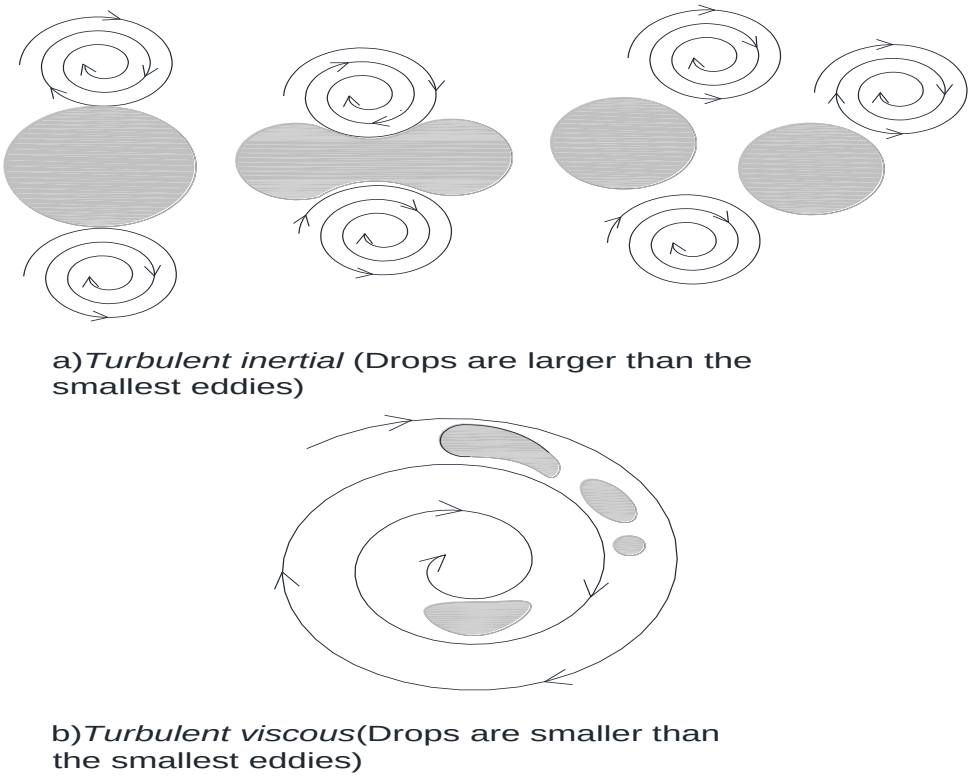

Figure 9: Schematic illustration of drops formation in turbulent flow under Turbulent inertial regime(a) turbulent viscous regime(b) (redrawn using AutoCAD 2018 from Rayner, 2015).

3.6.3 Fragmentation by cavitation

Cavitation is a complex phenomenon that occurs when fluid subjected to rapid changing in the pressure. The fluid shrinks arise when the pressure increase, or it extends as the pressure decrease. In HPH, the velocity of the pressurized fluid rapidly increases when it passes through the narrow gap, lead to low static pressure zone. As the static pressure acting on the fluid fall a critical value (below vapor pressure), vapor cavities begin to form. These cavities continue to grow with the fluid extension until the liquid pass into regions of higher local static pressure where these cavities collapse generating an intense shock wave which disrupts the surrounding drops, this phenomenon called hydrodynamic boiling, or cavitation (Håkansson,2015).

Innings among other founds that 15-20% of second stage pressure lead to avoid immoderate cavitation that leads to the formation of large cavities, which affect the homogenization effectiveness by increasing the gap height (Innings, 2005).

A dimensionless number is used to characterize the potential of the flow to cavitate known as Cavitation number (N_c). Cavitation number defined as the ratio of local absolute pressure from the vapor pressure and the kinetic energy per volume. In general, if the Cavitation number lower than the critical value, cavitation will occur, and it becomes denser as a result to decrease the Cavitation number (Håkansson, 2015).

Previous experimental works have indicated that cavitation likely occurs at the entrance of the homogenization valve due to the high local velocity generated at this narrow area (Phipps,1974) such a result is compatible with Håkansson researches. Håkansson has observed by visualizations of cavitation that the cavities collapse before exiting into the outlet chamber. Furthermore, wear measurements at the corner conform the entrance of the gap as a cavitation region. Wear measurements also suggested that cavitation located on the other side of the gap just before the entrance of the outlet chamber.

Fragmentation location can be used to indicate which breaking mechanism is dominated the HPH. Innings & Trägårdh have reported that break up occurs at the outlet chamber at 10–20 gap heights downstream of the gap (Innings & Trägårdh, 2005, 2007). Comparing the location of fragmentation and cavitation does not support cavitation as a dominant mechanism, and it is possible to conclude that cavitation causes drops deformation drops to a limited extent and drops fragmentation is a result of turbulence at the exit chamber of HPH.

3.6.4 Other fragmentation mechanisms

The previously discussed mechanisms suggested drops fragmentation occurs as a result of the interaction between the drop and the flow field. However, other mechanisms have been proposed, suggesting that break up is a result of friction between the particles and the solid surface of the homogenization valve itself.

First theory proposed that particles deformation caused by the direct collision of drops with the impact ring of the homogenizer due to the high jet velocity at the outlet

chamber, this theory is known as impingement theory (Kleinig & Middelberg, 1998; Engler & Robinson, 1981). Impingement theory has been refuted by the observation of drops fragmentation in HPH valve, which shows that fragmentation of particles placed in 10–20 gap heights downstream of the gap before they reach the impingement ring (Innings el al., 2011). Furthermore, measurement of exit jet velocity down steam of the gap has shown that jet velocity decrease with distance, and it becomes relatively low when the jet reaches the impingement ring (Innings & Trägårdh, 2007).

3.7 Cell fragmentation

Substantially less is known about cell or fiber breakup in high-pressure homogenizers compared to emulsion drop breakup, at least in terms of the fundamental breakup or mechanism. It is often assumed that one of the mechanisms suggested for drop breakup also controls cell and fiber breakup. However, since length-scales and material properties differ, it is not necessarily the same mechanisms that control fiber, cell and emulsion drop breakup.

Moreover, some studies suggest new mechanisms not often encountered in drop breakup literature. Most of the previous researches do not consider squeezing of emulsion droplets between the seat and the forcer as they pass through homogenization valve as breaking mechanism that because the small size of fat drops (3-5 µm) comparing to gap height of the homogenizer valve (Håkansson, 2015). However, squeezing can be discussed as a possible mechanism in the case of tomato suspensions due to the large size of tomato cells comparing to the gap opening of the homogenizer. The average diameter calculated of the tomato cells was 350 to 450 µm estimated by light microscopy (Lopez-Sanchez et al., 2011). The gap height of the bench top homogenizer range between 20-60 µm (optimum 50-60 µm). Comparing the cells size to the gap Hight indicates a significant difference in size between the gap height and cells size which could result in deformation of particles due to the interaction between the particles and solid surface of the valve.
Several researchers have investigated the potential of HPH to disrupt and inactivate bacterial cells in food and other products. Research into this type of applications has reported that inactivation of bacterial cells decreased with increasing fluid viscosity, which mean that higher serum viscosity leads to less homogenization efficiency (Diels et al., 2005, Coccaro, et al., 2018). The attempts to explain cells breakup also suggested impingement as breaking mechanism that leads to disruption of yeast cells rather than E. coli cells determined by a fluid dynamics computational model (Kleinig & Middelberg, 1996). Cells impingement rely on pressure at the collision point that depends on the velocity of the jet, the density of the fluid, the distance between the gap and the impingement ring as well as the jet diameter, which estimated to be equal to gap height (Moore et al., 1990), whereas that fluid viscosity has no influence on the impingement.

3.8 Hypothesis

The objective of this project was to investigate to which extent the previously proposed fragmentation mechanism explains fiber break up in the high-pressure homogenizer. Several hypotheses were formulated based on the different mechanistical suggestions to test which breaking mechanism is causing fragmentation of fiber in the homogenization valve. Table (1) summarizes how the particles size is expected to scale following each hypothesis.

If LV regime were dominating the fiber breakup, increasing of serum viscosity would decrease the drop size for the homogenizer juice with an expected slope value of -1, see equation (9). The relationship between pressure and d_{max} suggests that particles size is inversely proportional to pressure, see Appendix (A).

In TV regime smaller particles size can be obtained by higher continuous phase viscosity as is shown in the equation (15). If the TI mechanism would be the dominating mechanism, serum viscosity does not influence on particles break up in the HPH.

Correlation between maximum size and pressure hypothesizes that increasing of homogenization pressure would decrease the maximum particles size for homogenized tomato suspension with an expected slope of -1 and -4/5 for TV and TI regimes respectively, see Appendix(B).

Table 1: Expected particles size for each hypothesis.

Hypothesis	**Experimental action**	**Expected particles size**	**Expected slope**	**Equation**
LV	Increasing η_c	Decreasing d_{max}	$d_{max} \propto {\eta_c}^{-1}$	$d_{max} = \frac{2\gamma We_{cr}}{\eta_c G}$
	Increasing ΔP^*	Decreasing d_{max}	$d_{max} \propto \Delta P^{-1}$	$d_{max} = \frac{\gamma We_{cr}\rho_c}{\pi r_e \eta_c \Delta p}$
TV	Increasing η_c	Decreasing d_{max}	$d_{max} \propto {\eta_c}^{-1/2}$	$d_{max} = \left(\frac{\pi r_e}{10Q{\rho_c}^2}\right)^{-1/2} \Delta p^{-1} \gamma \eta_c^{-1/2}$
	Increasing ΔP^{**}	Decreasing d_{max}	$d_{max} \propto \varepsilon^{-1/2} \propto \Delta P^{-1}$	$d_{max} = \gamma \varepsilon^{-1/2} \eta_c^{-1/2}$
TI	Increasing η_c	No effect	-	$d_{max} \approx \varepsilon^{-2/5} \gamma^{3/5} \rho_c^{-1/5}$
	Increasing ΔP^{**}	Decreasing d_{max}	$d_{max} \propto \varepsilon^{-2/5} \propto \Delta P^{-4/5}$	$d_{max} = \left(\frac{\pi r_e}{10Q{\rho_c}^2}\right)^{-\frac{2}{5}} \Delta p^{-\frac{4}{5}} \gamma^{\frac{3}{5}} \rho_c^{-1/5}$
Squeezing	Changing gap height	converges to gap height	-	-

* Appendix (A) shown the relationship between the pressure and the particles size in LV regimes **See Appendix (B) shown the relationship between the pressure and the particles size in TV and TI regimes.

4 Material and method

4.1 Bench top homogenizer

Experimental works were performed using two stages benchtop homogenizer. The homogenizer designed by Tetra Pak and it has the same gap opening as production scale homogenizer i.e., the gap height is approximately 45 µm when operated at 150 bar and flow rate of 304 L/h. The homogenizer consists of a pump that delivers 38 ml of product with each piston stroke, and two homogenization heads as shown in Figure (10).

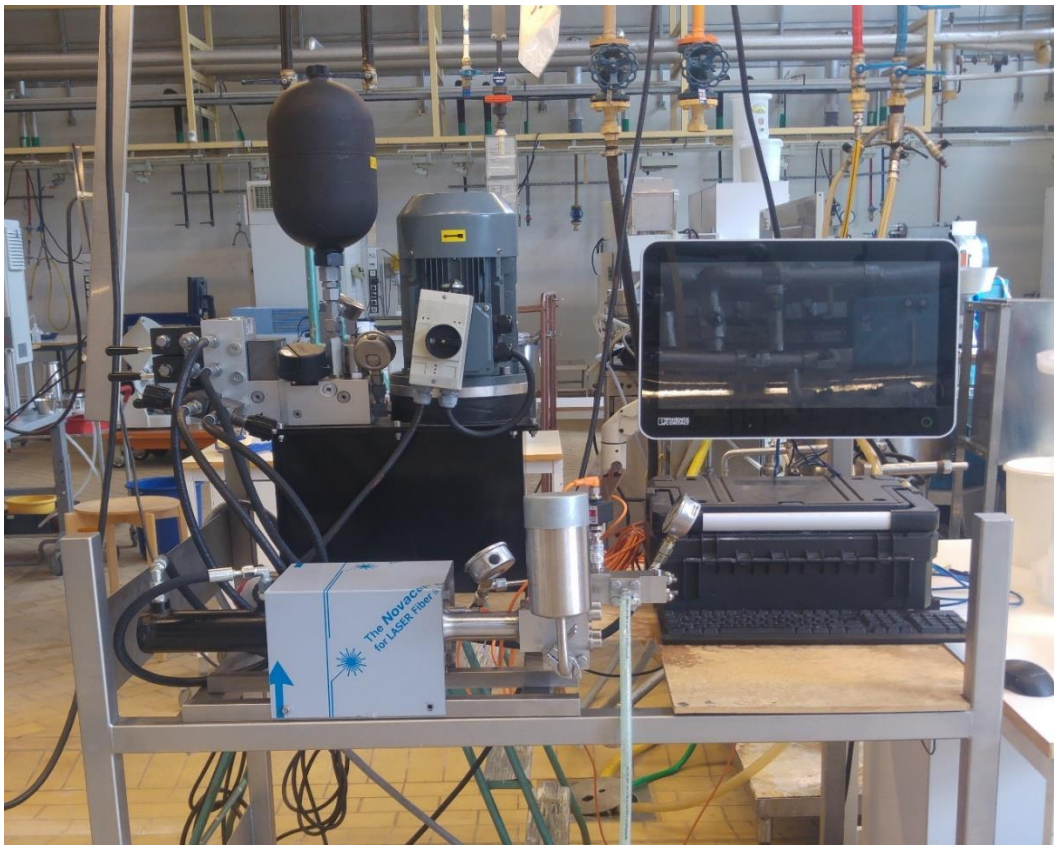

Figure 10: Benchtop homogenizer trail setup at chemical center, Lund.

The benchtop can create a wide range of homogenization pressure up to 500 bar and flow rate range between 6.8-342 L/h by changing the stroke time of the piston. The specification of the bench top homogenizer shown in Table (2).

Regular checking for the homogenization head was performed to avoid wearing forcer and seat due to the homogenization of such an aggressive product. Wear may decrease

the homogenization efficiency and prevent the machine from achieving high homogenization pressure.

Table 2: Geometry and properties for the bench top homogenizer (Tetra Pak internal system).

Description	Symbol	value	Unit
Flow rate	Q	6.8-342	L/h
Gap Inlet radius	r_i	1.5	mm
	r_{IC}	1.5	mm
Gap exit radius	r_e	2	mm
	r_{OC}	2	mm
Stroke time	-	0.4-1	s
Homogenization pressure	p	0-500	bar
Gap height	h	20-60	µm

4.2 Material

4.2.1 Raw material

Hot break tomato paste of concentration 28-30% (Sugal Group, Spain) was used in all experimental trials. The paste was purchased by Tetra Pak and has been stored in a 6˚C cool room, the specification of raw material is shown in Appendix H.

4.2.2 Juice preparation for investigation of the influence of several passages, gap height, and homogenization pressure

The hot tomato break was used for the preparation of the tomato juice that contains 18.8 % of tomato concentrate. The percentage of tomato concentrate was chosen base on the Brix value of commercial tomato juices, which had a Brix value equal to 4.9±0.1 Brix.

The juice preparation began with the dilution of tomato paste to the 4.9˚Brix level by mixing with cooled tap water with hand mixing until all tomato lamps dissolved. The Brix level was measured by a HI-96801 refractometer. Then samples were vacuumed to remove the air bubbles that could affect the hominization efficiency by using a Buechner flask and pipe water as a vacuum source. The samples vacuumed until the air bubbles exploded. After vacuuming, the juice was transferred to clean flasks and ready for homogenization.

In case of investigation of several passages' homogenization, only the juice with 9.2 % of tomato concentrate was used because the pretrial on 18.8 % of tomato concentrate

had caused drastic damage to the homogenization machine due to viscosity increasing of the homogenized juice with each passage.

4.2.3 Juice preparation for investigating of the influence of continuous phase viscosity

A serial of tomato juice with different continuous phase viscosity was proposed to investigate and understand the effect of serum viscosity on the homogenization of tomato suspension. It was suggested to use the serum phase viscosity values of the tomato juice concentrations shown in the table (3). After preparation of juice with a higher percentage of solids using the same method as in the previous sections, the shown procedure in section 3.2.4.1 and 3.2.4.2 was used for the proportion of tomato juice of different serum phase viscosity. Note that a higher percentage of tomato concentrate led to higher Brix level due to increasing the amount of the soluble fibers.

Table 3: Suggested tomato juices concentration for investigation of the influence of continuous phase viscosity

Tomato juice concentration %	**Brix level ±0.1**
9.2	2.4
18.8	4.9
28.4	7.4
38	9.8
45.7	11.9

4.2.4.1 Serum viscosity for tomato juice

In order to determine the serum viscosity of tomato juice, the tomato juice of different concentration was centrifuged using ultracentrifuge (Optima LE-80K, Beckman Coulter) at 11000g for 20 mins at 20°C using an SW41Ti rotor that can hold six tubes of 13.2 ml (tube diameter 14 mm). After centrifugation, the serum phase was separated from the solids using pipet.

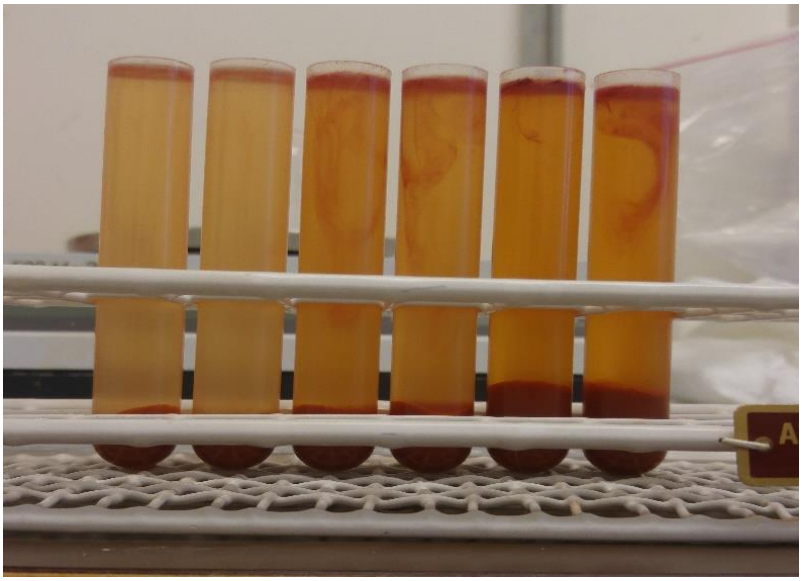

Figure 11: Centrifuged tomato juice that have different percentage of tomato concentrate.

Considering serum phase has shown a shear thinning behavior, it was suggested to use apparent viscosity at a shear rate equal to 10 s^{-1}(see section 3.3.2.3 which explains the method used to determine the apparent viscosity). The serum viscosity of tomato juice increased with the percentage of tomato concentrate, and the 9.2% of tomato concentrate has the lowest value of apparent viscosity as shown in Figure (12). The estimated apparent viscosity values represent the target apparent viscosity values that should be achieved by adding sugar to tomato juice of 9.2% of tomato concentrate.

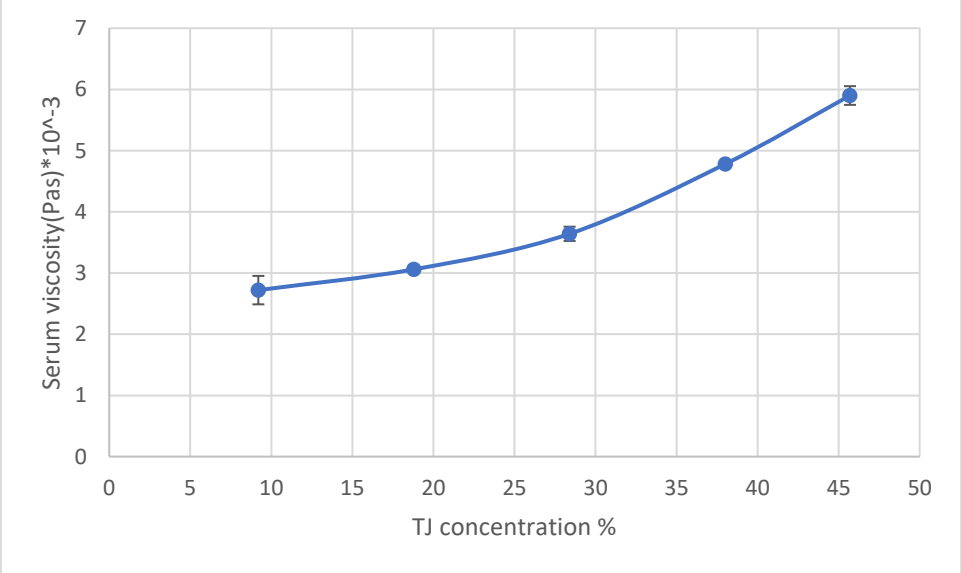

Figure 12: Apparent viscosity values of TJ of different percentage of tomato concentrate at shear rate 10 s^{-1}. The error bar represents 2± stander error.

4.2.4.2 Estimation of the required amount of sugar

In order to rich higher serum viscosity of the samples, sugar was added with using the same volume fraction of the dispersed phase. Estimation of the required amount of sugar started with the dilution of sugar in hot water and cooling it down again. The percentage of sugar added, and the included amount of water are shown in the table (4).

Table 4: Formulation for tomato juice with randomly chosen sugar concentration.

TJ concentration %	Sugar %	Water %	sugar solution %
9.2	0	90.8	90.8
9.2	5	85.8	90.8
9.2	10	80.8	90.8
9.2	15	75.8	90.8
9.2	20	70.8	90.8
9.2	25	65.8	90.8
9.2	30	60.8	90.8
9.2	35	55.8	90.8
9.2	40	50.8	90.8

Next, tomato juice concentration of 9.2% was mixed with the sugar solution using a simple wire whisk. Finally, juice was centrifuged, and serum viscosity was measured as described for tomato juice serum without sugar. All measurement was duplicated.

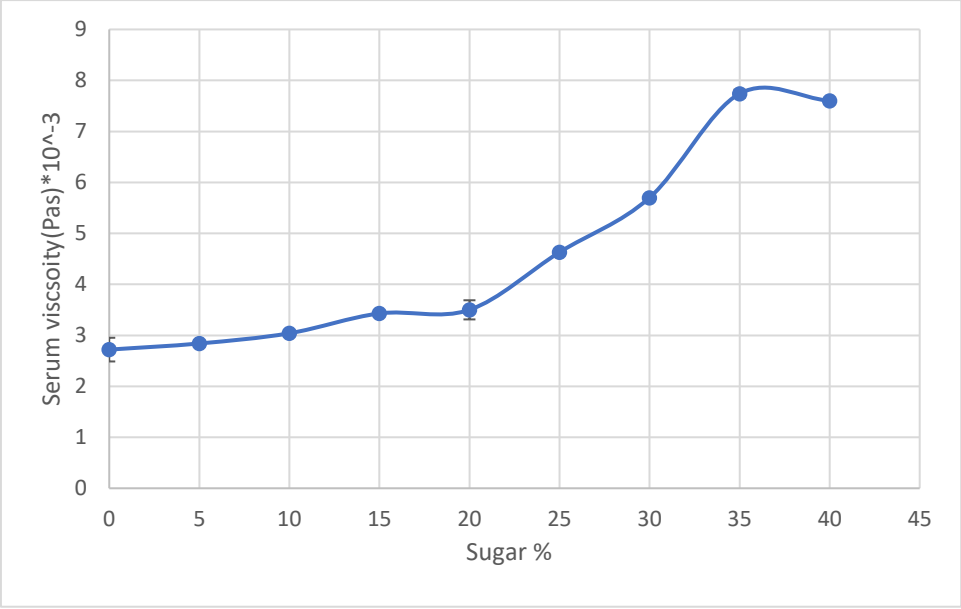

Figure 13: Serum viscosity at shear rate of 10 s^{-1} as a function of added percentage of sugar to TJ of 9.2% of tomato concentrate. The error bar represents 2± stander error.

By applying the target serum viscosity values on Figure (13), the needed amount of sugar was estimated. Not that Linear interpolation was used to obtain a better-approximated value for the sugar percentage. The calculated percentage of sugar that used in juice preparation for investigating the effect of increasing serum viscosity are shown in Table (5).

Table 5: Formulation of tomato juice that used in investigating of the influence of continuous phase viscosity.

TJ concentration%	**Target serum viscosity (Pas)×10^{-3}**	**Sugar concentration%**
9.2	2.72	0
9.2	3.07	10.28
9.2	3.6	20.59
9.2	4.8	25.67
9.2	5.9	30.48

Juice was prepared as explained before with adding the desired amount of sugar and ready to be homogenized.

4.3 Experimental procedure

4.3.1 Experimental design

4.3.1.1 Investigation of the influence of homogenization pressure

In most of the food application, two stages homogenization is usually applied. It is common to use 20% of homogenization pressure in the second stage, although there is no clear evidence regarding the contribution of the second stage to the breakup of particles in HPH. The second stage homogenization pressure was fixed to 20% of the first stage pressure. The suggested combination of pressure shown in Table (6).

Table 6: Experimental matrix for the investigation of the influence of homogenization pressure. The shown pressures represent the first stag pressure and the second stage pressure is 20% of the first stage pressure.

Investigation the influence of the homogenization pressure					
TJ%	**Pressure**				
	0bars	50bars	100 bars	200bars	300 bars
9.2	√	√	√	√	√
18,8	√	√	√	√	√

After homogenization, the used hydraulic and homogenization pressures were documented, and homogenized samples are ready for further analyses.

4.3.1.2 Investigation of the influence of several passages

Base on the juice experts in Tetra Pak, most of the consumers, prefer juices with homogenization pressure around 150 bar on the first stage and 30 bar (20%) on the second stage. However, in this stage the machine was shown some limitation (vibration) when it was operated at 30 bar (20%), thus the second stage homogenization pressure was reduced to only 14% (20bar) of the second stage was used. The experimental matrix is shown in Table (7). Note that the juice was recycled until it reaches to the desired number of passages to prevent in the incorporation of the air bubble that may affect the homogenization efficiency.

Table 7: Experimental matrix for the investigation of the influence of several passages.

Investigation the influence of the several passages							
TJ%	**Several passages**						
	0NH	NH	2NH	4NH	8NH	16NH	32NH
9.2	√	√	√	√	√	√	√

4.3.1.3 Investigation of the influence of continuous phase viscosity

In this part of investigation homogenization pressure fixed to 150 bar for the first stage and 20 bar for the second stage. Various amount of sugar was added to tomato juice of 9.2% tomato concentrate to achieve higher continuous phase viscosity, see Table (5) that shows the formulation of tomato juice used for investigation.

Table 8: Experimental matrix for the investigation of the influence of continuous phase viscosity.

Investigation of the influence of continuous phase viscosity					
TJ%	**Serum viscosity**				
	$2.72*10^{-3}$ Pas	$3.07*10^{-3}$ Pas	$3.6*10^{-3}$ Pas	$4.8*10^{-3}$ Pas	$5.9*10^{-3}$ Pas
9.2	√	√	√	√	√

4.3.1.3 Investigation of the influence of gap height

The influence of the gap height on the breakup of fibers was tested by changing gap height value that obtained by varying the flow rate of the machine. Base on the machine ability three values of flow rate was selected, and the responding gap height values calculated as shown in Appendix(F). The homogenization pressure is 150 bar for the first stage and 20 bar for the second stage.

Table 9: Experimental matrix for the investigation of the influence of gap height.

Investigation the influence of gap height			
TJ%	**Gap height**		
	45 µm	34 µm	26µm
9.2	√	√	√
18,8	√	√	√

4.3.2 Analytical method

4.3.2.1 Microscopy

The effect of homogenization on tomato juice samples was examined by using a light microscopy (Olympus BX50 F4, Olympus Optical CO, Japan) with a magnification level of 5X. The samples were placed on glass using a pipette and carefully covered with a cover glass. After adjusting the samples, clear images were taken using attached Sony digital camera and image software IC-Capture. Then ImageJ was used to set a scale bar upon the saved imaged.

4.3.2.2 Particle size distribution

The particles size measurement (PSD) was conducted using laser diffraction analyzer (Mastersizer 2000, Malvern UK). Data were analyzed using the Mie model which assumed that particles have a spherical shape. The average reflective index of plant cells was set to 1.42 with adsorption of 0.2 (Gausman et al., 1974). The stirring speed was used to be 1500 rpm. After setting the samples in the master sizer, one-minute waiting time was used to make sure that samples dispersed within the MiliQ water. Three measurements were taken for each sample by recording both the individual and the average of them. The particles size obtained a base on the volume or the area occupied where area-based diameter(D_{32}) and the volume-based diameter (D_{43}) respectively.

$$d_{32} = \sum_i n_i \, d_i^3 \, / \sum_i n_i \, d_i^2 \qquad \text{(Eq.16)}$$

$$d_{43} = \sum_i n_i \, d_i^4 \, / \sum_i n_i \, d_i^3 \qquad \text{(Eq.17)}$$

The area-based diameter determined by smaller particles in the system. The suspension volume-based diameter specified by the large particles present in the suspension (Goodwin, 2009; Bayod, 2008). Therefore, it was decided that the best method to adopt for this investigation was to use volume-based diameter since all the breaking mechanisms make predictions on the size of the largest surviving particles size i.e. d_{max}.

4.3.2.3 Rheology measurements

Rheology measurements were measured by Malvern Kinexus Pro viscometer with a four-bladed vane(d=21mm) and a regular cylindrical cup(d=25) that results in a gap height 2mm which can be considered suitable for large particles of the fiber suspensions. Several studies have shown that using vane geometry necessary to avoid slipping phenomenon. After loading the samples in the viscometer, samples were left to stabilize in 5 min before preforms the measurements to avoid time dependence

effect. Steady shear testing was used, the shear rate ranges from 10^{-4} to 100 s^{-1} at 20° C, and about 49 points were determined. The obtained date was moved to MS office for further analyses.

The juice serum was obtained by centrifuging, was subjected to same procedure with using a concentric cylinder as an upper geometry.

4.3.2.3.1 Analyzing viscosity

The apparent viscosity at a shear rate value of 10 s^{-1} was estimated from the obtained rheology date using two-point interpolation. The reason for using this value of shear rate was to make sure that samples reach to flow point, as well as some literature studies estimated the shear deformation of fluid food during oral processing is correspond to 10 s^{-1} (Chen & Stokes, 2012).

4.3.2.3.2 Yield stress

Yield stress represents the lowest shear stress value needed to create flow. Yield stress obtained by using tangent analysis as shown in Figure (14), the red line represents the yield stress value that obtained by applying tangent between the linear viscoelastic region (the horizontal line) and the flow region (the slope) and the crossing point of these tangents representing the yield stress value.

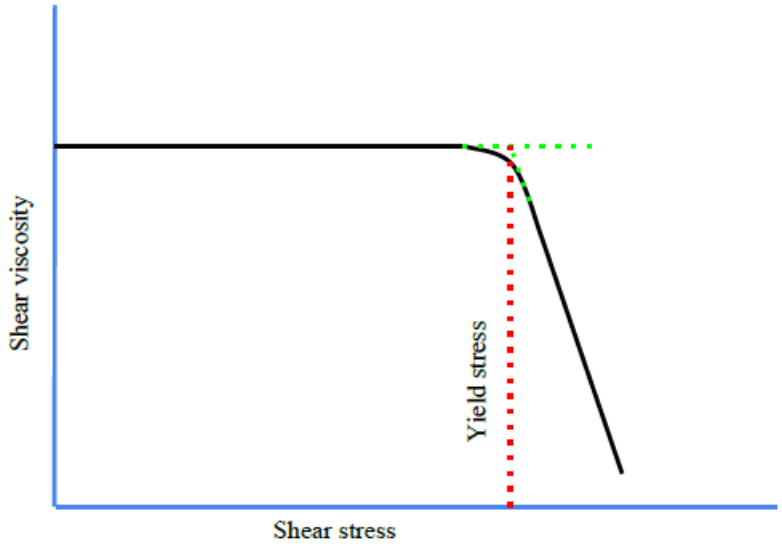

Figure 14: Illustration shows determination of yield stress by tangent analysis using steady shear testing (redrawn using Google Drawing from Panalytical, 2018).

4.3.3 Statistical analyses

One-way Analysis of Variance (ANOVA) was evaluated using MS Excel. The analyses were carried out on particles size results obtained by different gap height. The reason for performing this type of analyses to check whether there is a significant difference between the groups or not. The null (H_0) and alternative (H_a) hypotheses were set up in the following way:

H_0: $\mu_1 = \mu_2$, which hypothesizes that the mean values of particles size obtained from different gap height are equal.

H_a: not all μ are equal, which hypothesizes that not all the mean values of particles size obtained from different gap height are equal.

Using 95 % of confidence interval (α= 0.05), the null hypothesizes is rejected when P value $\leq$ α which mean that there is a significant difference between the samples.

Confidence Intervals for a single slope in simple linear regression was estimated using the data analysis function in MS Excel. The analysis was executed on the results obtained by changing the homogenization pressure as well as changing the continues phase viscosity. Using 95 % of confidence interval (α= 0.05), a confidence interval for single slope can be calculated by:

$$Confidacne\ interval = (estimated\ slope) \mp (t - critical\ value)_{(standard\ error\ of\ the\ slope)} \quad \text{(Eq.18)}$$

With degree of freedom of n-2.

5 Result and discussion

5.1 Investigation of the influence of homogenization pressure

At this part of the investigation, the influence of homogenization pressure was tested on tomato juice with 9.2% of tomato concentrate and tomato juice with 18.8% of tomato concentrate. The homogenization pressure was changed between 0 and 350 bar for the first stage and 20% of first stage homogenization pressure was used in the second stage.

5.1.1 Particles size

The unhomogenized tomato juice (0 bar) has the largest volume-base average diameter of 303 µm. The result in Figure (15) indicates that the mean volume base diameter decreases with increasing the homogenization pressure. The homogenized juice of 18.8 % of tomato concentrate has D_{43} between 283.6 and 85.7 µm for pressure ranges between 50 bar and 350 bar. The lowest volume-base average diameter of 9.2% of tomato concentrate obtained at the highest homogenization pressure. These results indicate that tendency of particles to break up increase with increase the homogenization pressure.

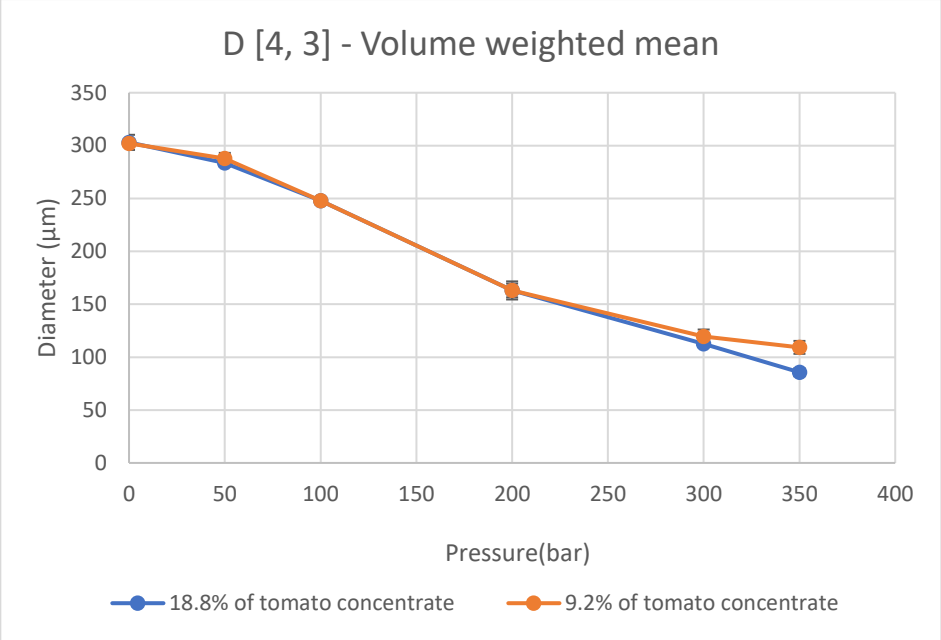

Figure 15: Volume weight mean D_{43} of TJ as function of homogenization pressure. The error bar represents 2± stander error.

The value of the slope of homogenized tomato juice of 18.8% is -0.599 found by plotting log D_{43} vs. log P, resulting in a slope of -0.523 in the case of 9.2% tomato juice as shows in Figure (16). The results of the surface base average diameter are shown in Appendix(C). The 95% confident interval of the slope is between -0.93 and -0,26 for 18,8% homogenized tomato juice and slope confidence interval of -0,76 and-0,29 for homogenized tomato juice of 9,2% solids, see Appendix(C).

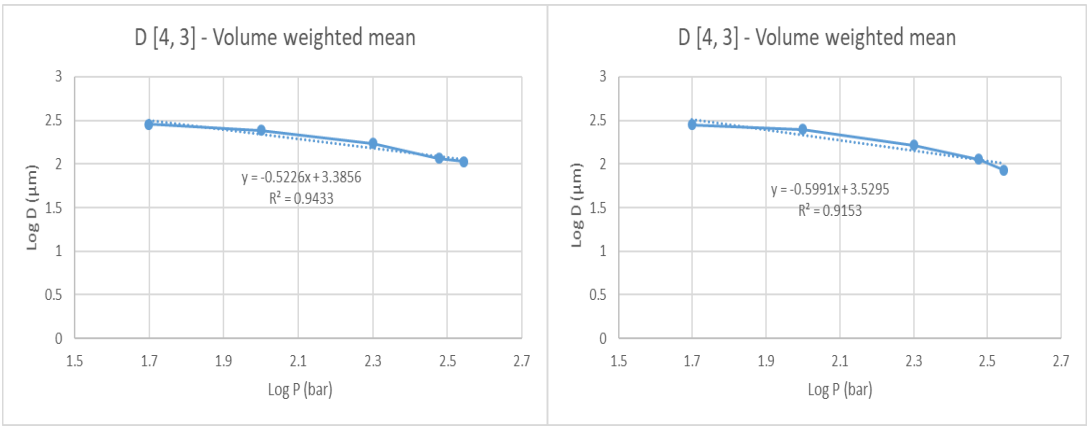

Figure 16: Log D_{43} as function of Log P of TJ (left)9.2% of tomato concentrate (right)18.8% of tomato concentrate.

For the particle size distribution, it reasonable that the unhomogenized sample has the largest size. As the homogenization pressure is applied the distribution is shifted towards more distinct bimodal distribution, and the peak is shifted toward the left as is

shown Figure (17). When applying a homogenization pressure at of 350 bar, the main peak can be seen at 79.4 µm, which complies with the average in Figure (15).

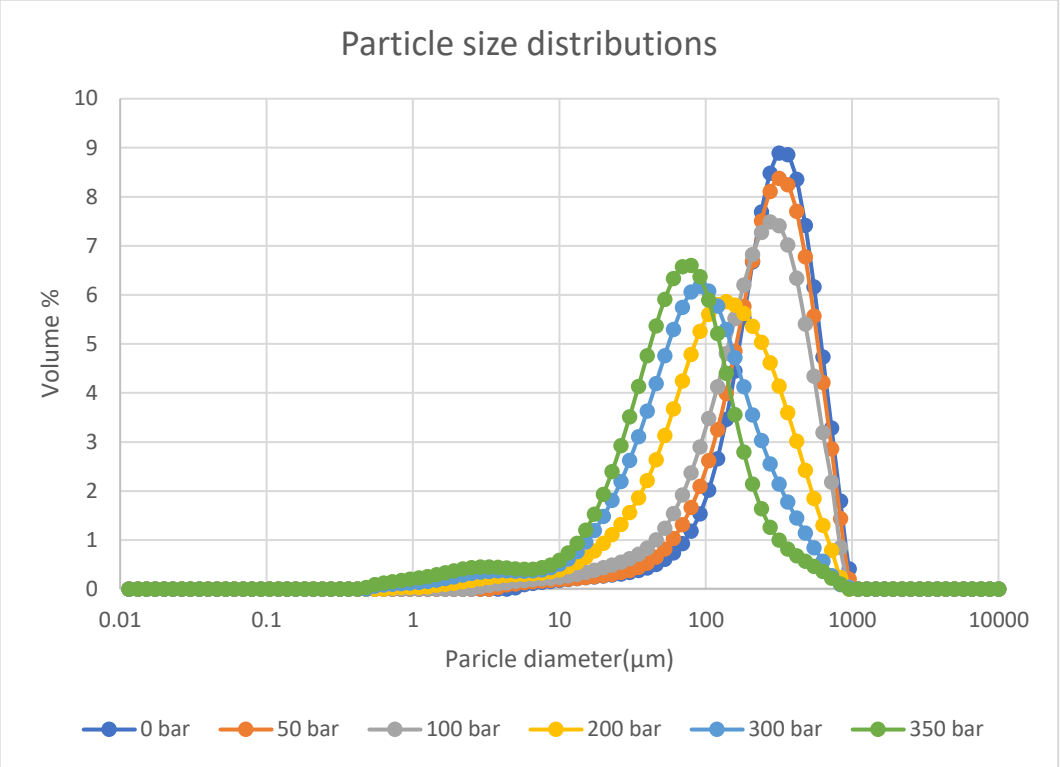

Figure 17: Particle size distributions of 18.8%TJ suspensions treated at different homogenization pressures.

5.1.2 Microscopy

In Figure (18), the microstructure of unhomogenized and homogenized tomato suspension can be compared. The picture of the unhomogenized sample reveals the presences of whole tomato cells with an approximate diameter of more than 250 µm. With increasing the pressure at 100 bar, the cells break up is started and picture shows a combination of some surviving cells, damaged cells and cell wall fragments. As the pressure is continuing to increase, the particles size continues to decrease rapidly, and only cells fragment are shown with no more extended present for tomato cells, indicating a higher tendency for breakup under higher homogenization pressure. The change in the structure appears to correlate well to the obtained particle sizes measurements.

unhomogenized TJ

Homogenized TJ at 100 bar

Homogenized TJ at 150 bar

Homogenized TJ at 350 bar

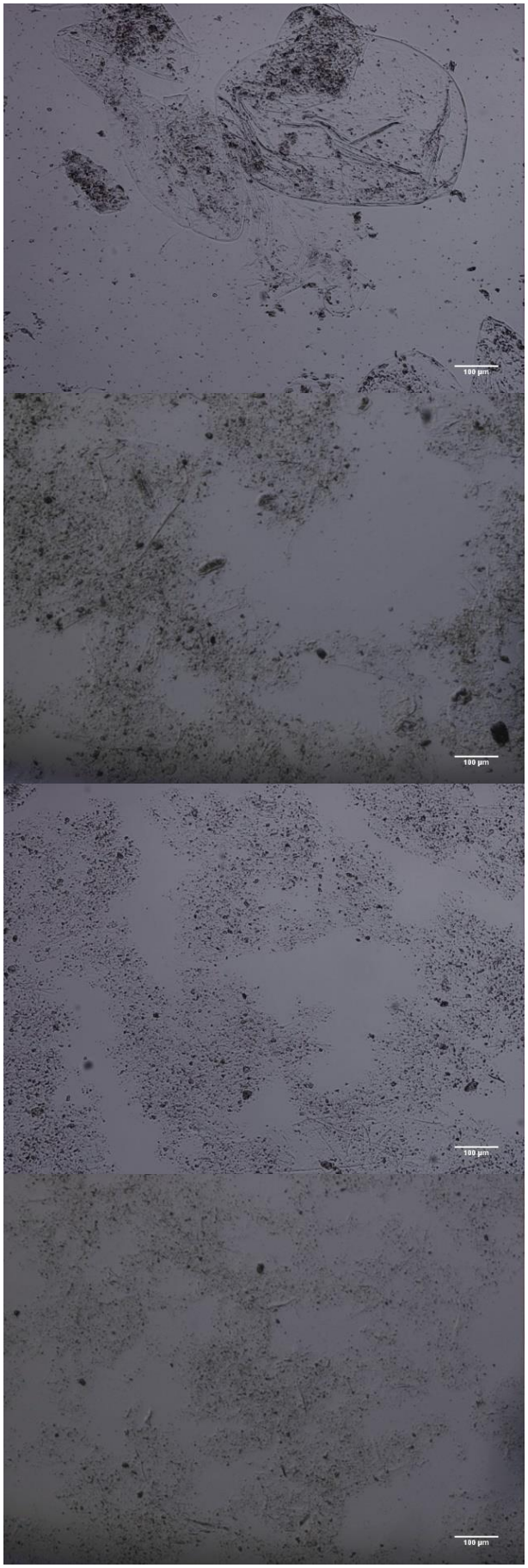

Figure 18: Comparing microstructure of unhomogenized tomato juice and homogenized tomato juice at different first stage homogenization pressure and 20% second stage homogenization pressure. The stander bar is 100 µm.

Microscopic images were taken from undiluted samples to avoid change of structure and try to get the nearest image of the structure before and after the homogenization. However, stirring during samples preparation may cause some breaking and change of the structure for a certain extent. Furthermore, each picture represents a part fiber network should be taken into consideration.

5.1.3 Rheology measurements

Rheology measurements of 18.8% tomato juice after homogenization is shown in Figure (19). The unhomogenized samples have the lowest apparent viscosity at 10 s^{-1} and yield stress value of 0.316 Pas and 0.073 Pa, respectively. As the homogenization pressure increase to 50 bar, the apparent viscosity increases to 0.618, and it continues to increase with increasing pressure. From the data in Figure (19), it is apparent that the yield stress of the unhomogenized sample is increased with homogenization pressure and higher homogenization pressure leads to higher yield stress.

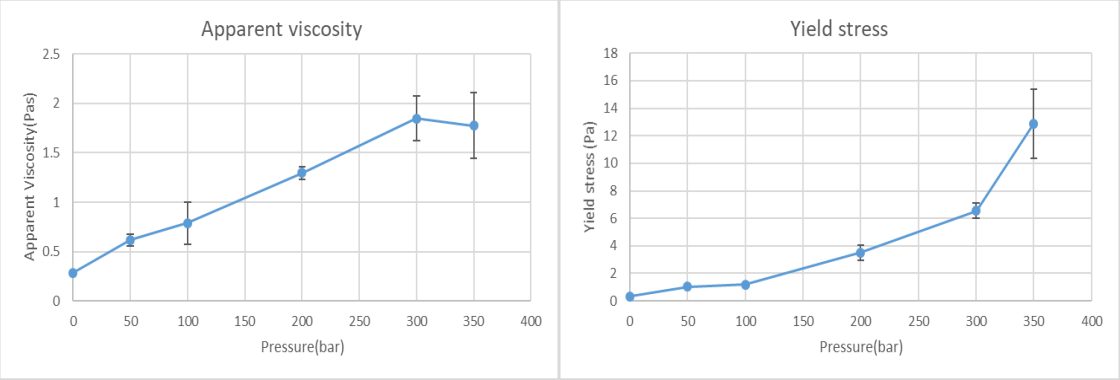

Figure 19: Apparent viscosity at shear rate of 10 s^{-1} and yield stress of 18.8% homogenized tomato juice as function of homogenization pressure. The error bar represents 2± stander error.

These changes in rheology properties match with the results of particles size as well as the change of structure shown by microscope. The reason for this behavior is that unhomogenized samples have the largest fiber particles, which are randomly arranged with a loose interaction between them, while the increase in the hominization pressure results in smaller fiber particles with higher number of particles that start to tangle and interact with each other and form a network. This network resists the applied force on the fluid resulting in higher viscosity and yield stress.

5.2 Investigation of the influence of continuous phase viscosity

The approach in this part of the investigation is to check the effect of increasing continuous phase viscosity on the particles' fragmentation of tomato juice in HPH. The continues phase viscosity was increased by adding varying amounts of sugar. The homogenization pressure was kept constant at 150 bar (first stage) with 20 bar for the second stage. In this section the characterization of rheology will not be included, due to sugar addition to the samples that leads to higher apparent viscosity and yield stress, thus comparing of samples will not be helpful.

5.2.1 Particles size

The results obtained from the preliminary analysis of particles size are shown in Figure (20), the samples that have lowest serum viscosity have the lowest volume-base average diameter of 198.3 µm. As the Serum viscosity increase, the tendency of HPH to break up the particles becomes lower resulting higher particles size. The sample of 5.9×10^{-3} Pas less affected by hominization pressure and has volume-base average diameter of 237 µm. In summary, these results show that higher continuous phase viscosity results in larger particles size. The value of the slope is 0.22 that is obtained from Figure (20). The 95% confident interval of the slope is between 0,148 and 0,292, as shown in Appendix (D).

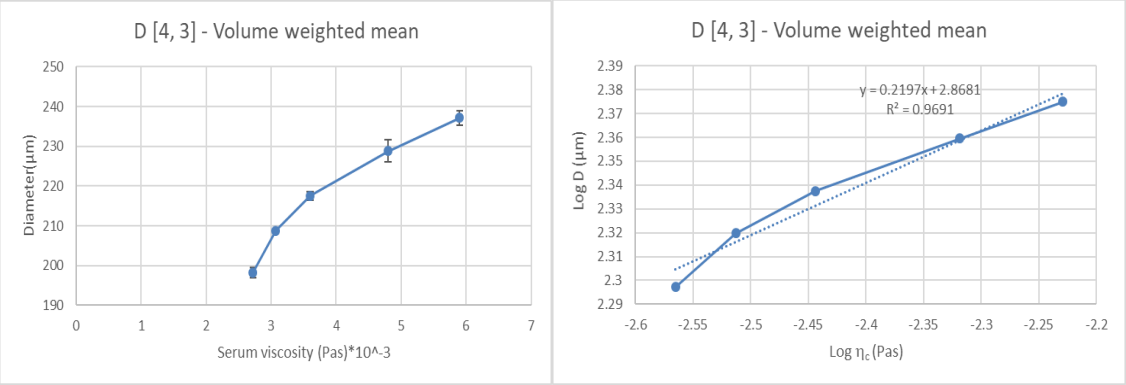

Figure 20: The influence of serum viscosity on volume weight mean D_{43} of homogenized tomato juice. The error bar represents 2± stander error.

The results of surface-based mean diameter D_{32} shows the same behavior as D_{43}, and the mean diameter increased by increasing the continuous phase viscosity, the results shown in Appendix (D).

Although, the difference of size distribution between the samples is a small, comparing the samples that have the highest serum viscosity with the one that has lower viscosity shows decreases the size fraction of the largest particle group and main peak shifting towards lower particles diameter.

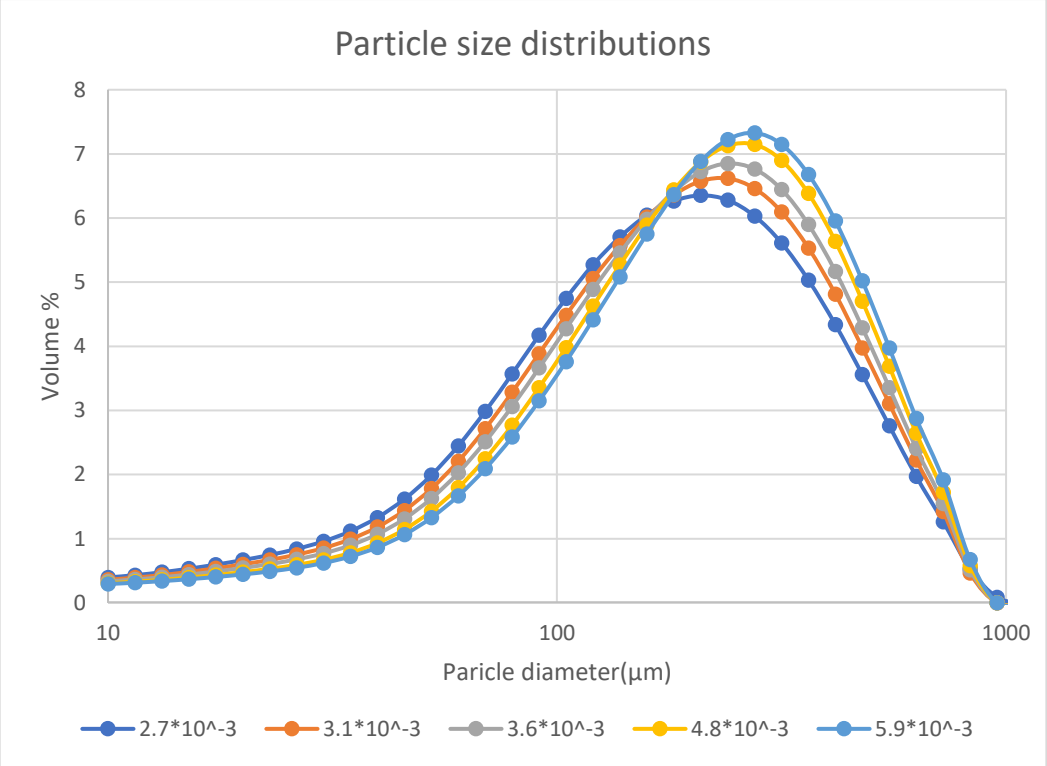

Figure 21: Particle size distributions of TJ of different continuous phase viscosity.

5.2.2 Microscopy

The pictures obtained by light microscopy for tomato juice with different continuous phase viscosity is shown in Figure (22). The homogenized samples of 2.7×10-3 Pas serum viscosity is shown small particles size and more even distribution of particles as result of homogenization treatment.

Homogenized TJ of 2.7× 10^{-3} Pas serum viscosity

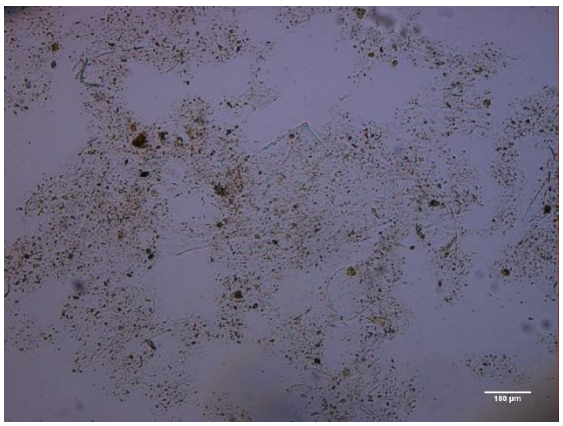

Homogenized TJ of 3.1× 10^{-3} Pas serum viscosity

Homogenized TJ of 3.6× 10^{-3} Pas serum viscosity

Homogenized TJ of 4.8× 10^{-3} Pas serum viscosity

Homogenized TJ of 5.9× 10^{-3} Pas serum viscosity

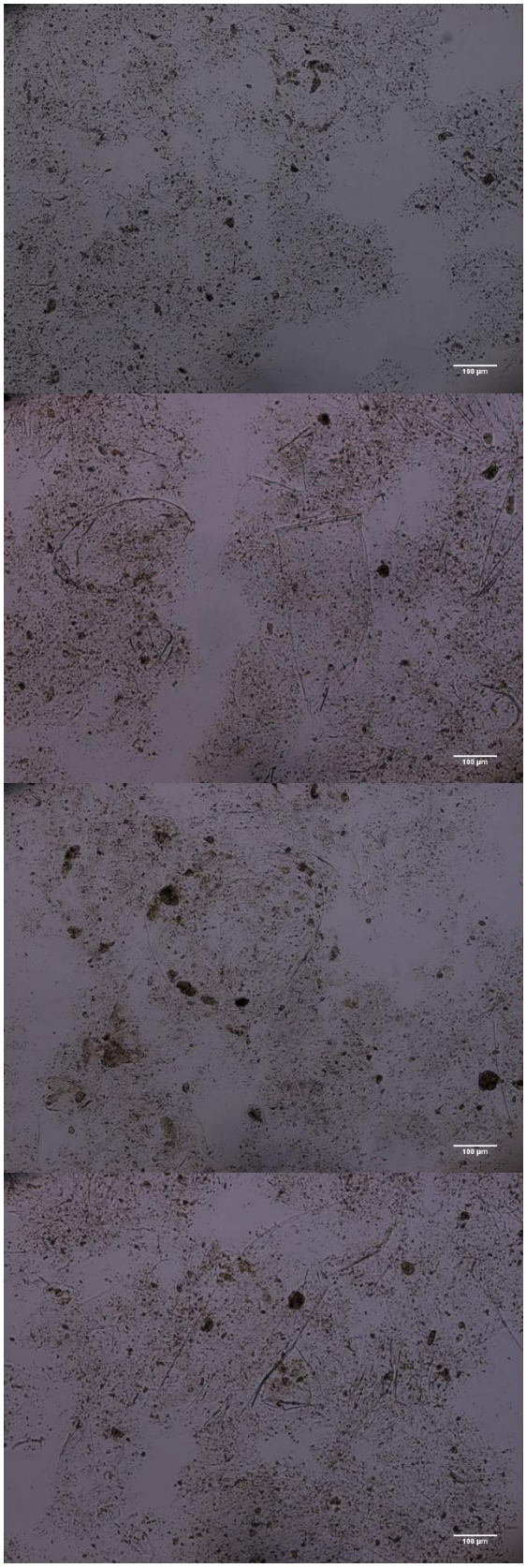

Figure 22: Influence of homogenization on the microstructure of tomato juice of different continuous phase viscosity. The standard bar is 100 µm.

while the pictures above for the treated samples with highert serum viscosity shows an uneven distribution compose from some big survived cells, cells fragment and residues of cells wall. This result refers that the homogenization efficiency decreased by increasing the serum viscosity leading to some unaffected cells. This observation is compatible with results obtained by the size distribution which showed a bigger particles size for higher serum viscosity.

5.3 Investigation of the influence of gap height

In this part of the investigation, the only variable that has been changed is the flow rate which results in different gap height: 45,34, and 25 µm. The homogenization pressure is 150 bar for the first stage and 20 bar for the second.

5.3.1 Particles size

The influence of gap height on particles size is shown in Figure (23). In case of 18.8%TJ, the volume-based average diameter resulting from the highest gap is 219µm, while the lowest gap height results in an average diameter of 225.8 µm, which indicates that gap height cause no variation in the particles diameter of homogenized juice.

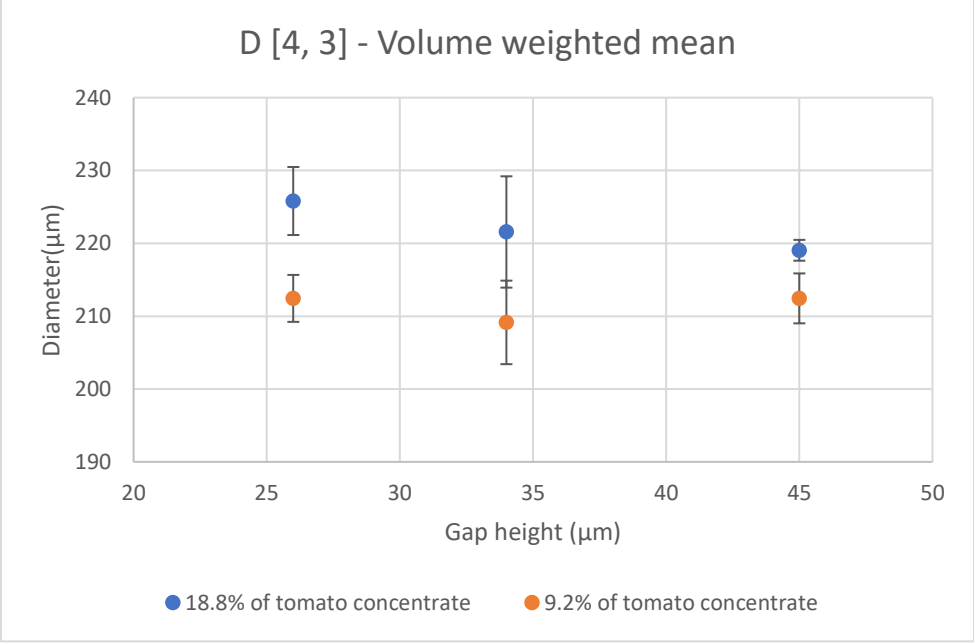

Figure 23: Influence of gap height on volume weight mean D_{43} of homogenized 18.8% and 9.2% of tomato juice. The error bar represents 2± stander error.

From the output of the one-way ANOVA analysis, see Appendix (G), the gap height shown no statistical difference between the resulting diameter of the homogenized juice. The obtained p values are 0.235 and 0.343 for D_{43} and D_{32}, respectively.

Testing tomato juice of 9.2% demonstrates no clear trend of gap height on the surface or volume base diameter and this observation was consistent with the results for ANOVA analysis of D_{43} and D_{32} as shown in Appendix (G).

It should be noted that the homogenization pressure in the HPH is not fixed instead it has a small variation with each stroke which can explain the variation in the obtained diameter of the homogenized juice.

5.3.2 Rheology measurements

As mentioned before, the rheology measurements reflect particle size of the tomato fiber, smaller fiber particles lead to higher viscosity, and yield stress or large particles lead to smaller values of viscosity and yield stress. Figure (24) shows the influence of gap height on the rheology of homogenized tomato juice of 18.8 %. The results shown no evident effect of the gap height on viscosity and varies from 1.208 to 1.33 Pas when changing the gap height from 45 to 26 µm. Yield stress as well is showed no differences with the gap height.

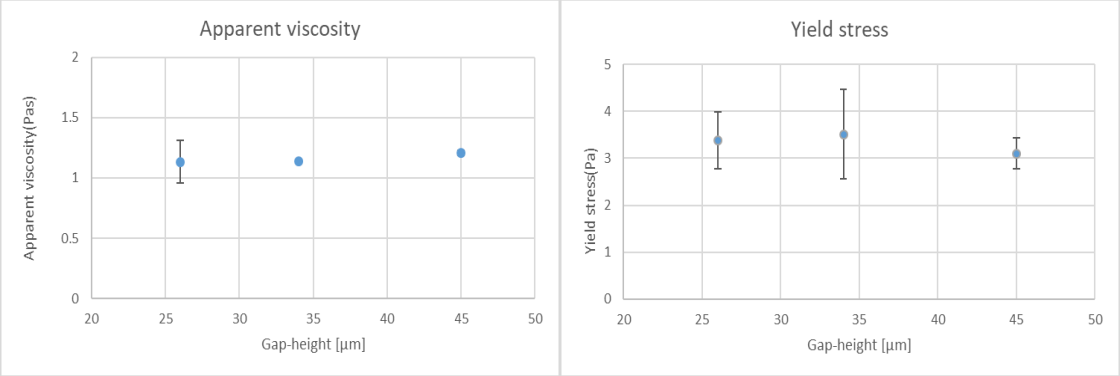

Figure 24: Apparent viscosity at shear rate of 10 s^{-1} and yield stress at different gap height for 18.8% of tomato juice. The error bar represents 2± stander error.

The same behavior was noticed by 9.2% homogenized tomato juice as shown in Appendix (G). These results match with results obtained by light diffraction showing no influence of gap height on the particle size in the HPH.

5.4 Investigation of the influence of several passages

The tomato juice of 9.2% was homogenized for several times at 150 bar first stage homogenization pressure and 20 bars for the second stage, samples were withdrawn after homogenization for 0 ,1, 2, 4, 8, 16 and 32 of passages.

5.4.1 Particles size

The unhomogenized sample has the largest volume-base average diameter of 303 µm. Homogenization of tomato suspension resulting in smaller particles size as provides in

Figure (25), the most significant part of particles size lost in the first two passages and the particle diameter reach to 115 µm. After 32 times homogenization, particles continue to break up, and more passages will be needed to reach a point where no break up occurs.

It is possible to notices that volume-based average diameter is reached a value of 21.5 µm after 32 passage which can be considered as extremely low value comparing to the gap height that has a value of 45 µm.

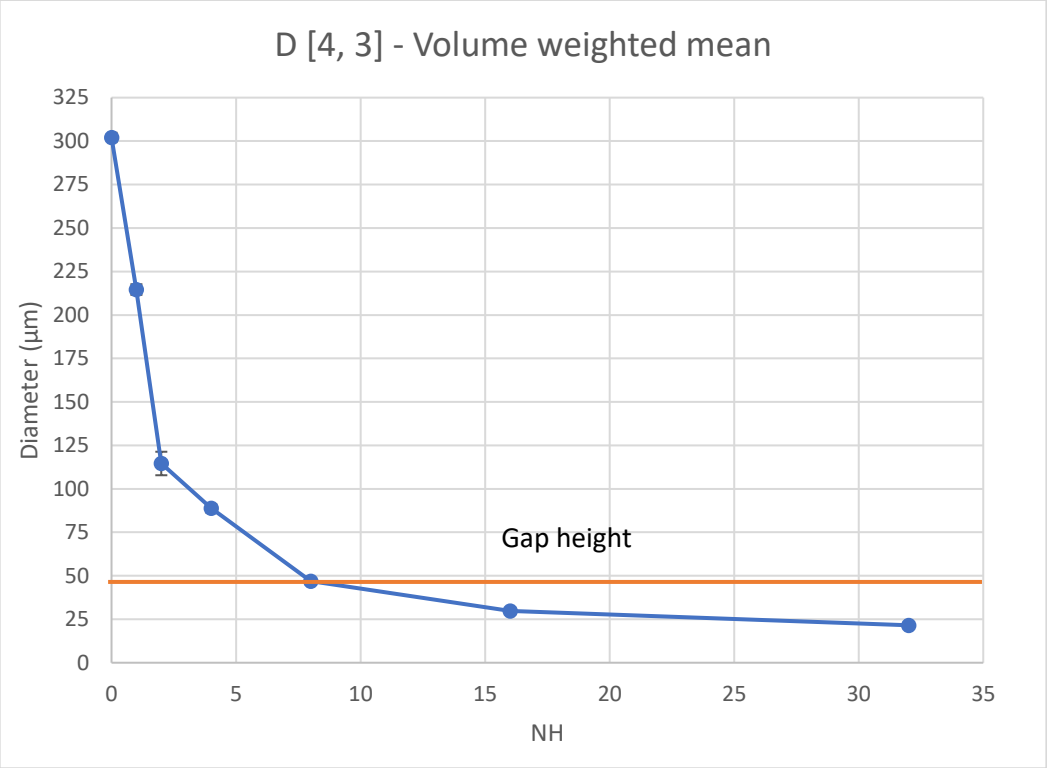

Figure 25: The Influence of several time homogenization on the volume base mean diameter D_{43}. The error bar represents 2± stander error.

The surface base diameter results are shown in Appendix E. The highest surface mean is for unhomogenized tomato juice which has value of 143.865 µm. The surface base dimeter reaches to value of 12.599 µm. After the second passage. Then, the fragmentation continues to occur with less intensity, but it does not stop even after 32 passages.

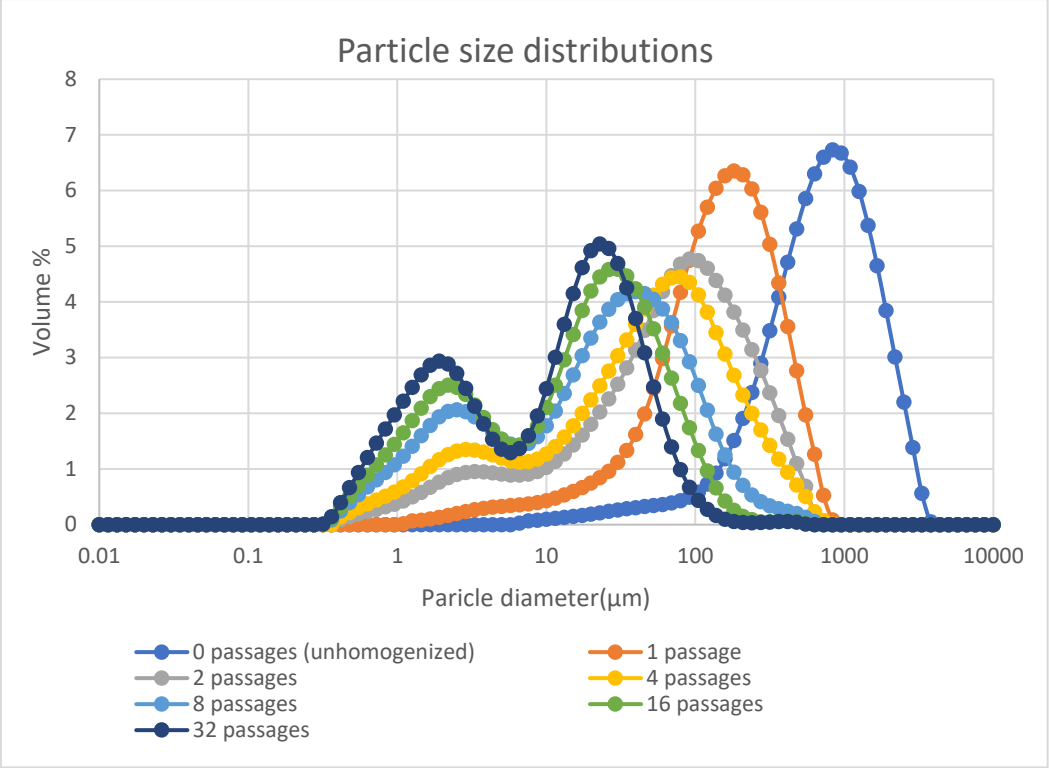

Figure 26: Particles size distribution of the 9.2 of homogenized tomato juice treated for several passages.

The particle size distribution of the measured samples is shown in Figure 26. It can seem that unhomogenized and one homogenized passage samples exhibit a more unimodal distribution. Homogenization with two and more distribution shifted towards bimodal distribution as there is increasing of the particles fraction of size less than 10 µm. Thus, the treated samples for 32-time passage observed two beaks in 25 µm and 2 µm.

5.4.2 Microscopy

Figure (27), shows the influence of homogenizing the tomato juice with several passages. Observed particles in the picture appears to match the measured particle size distributions very well. As discussed before, it is possible to notice whole tomato cells for the not, and one passage homogenized juice. After the second the passage, only cells wall fragmented is present with no longer exist for the tomato cells.

unhomogenized TJ

1 passage homogenization of TJ

2 passages homogenization of TJ

8 passages homogenization of TJ

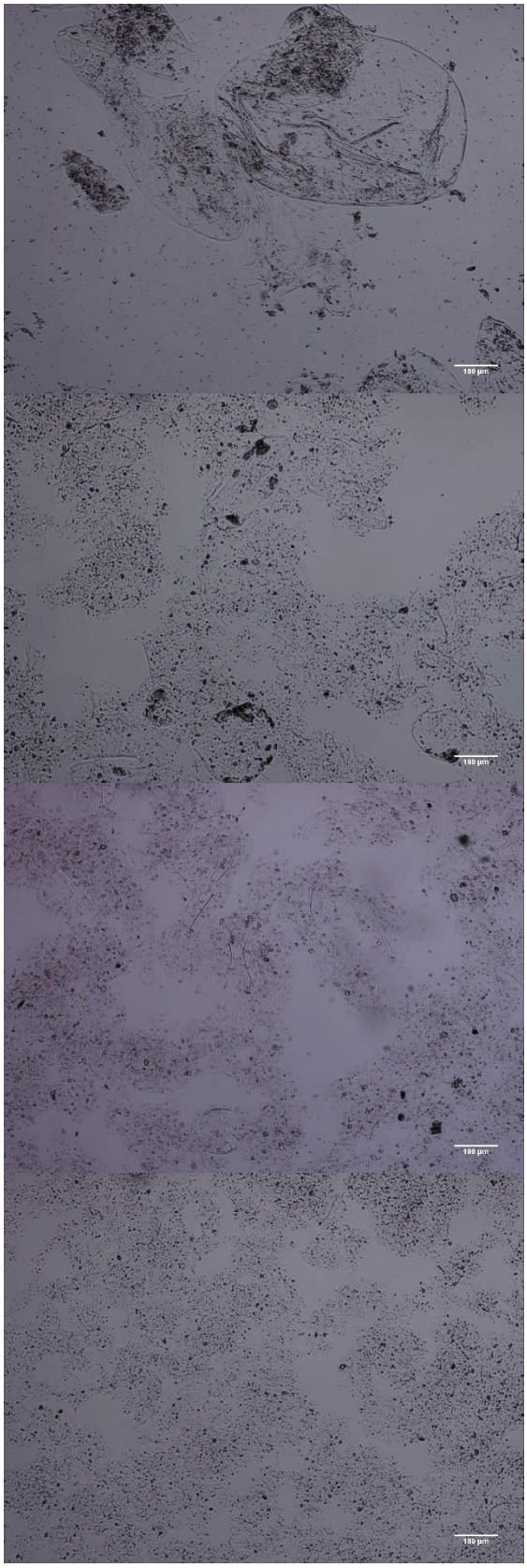

32 passages homogenization of TJ

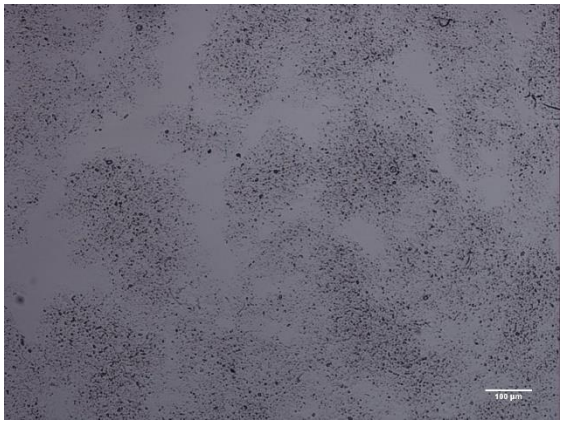

Figure 27 : Comparing microstructure of TJ after several passages' homogenization. The standard bar is 100 µm.

Then, the particles continue to break up with higher passage number and smaller particles size obtained. The homogenized juice of 32 times has the smallest particles size achieved.

5.4.3 Rheology measurements

As expected, the unhomogenized samples of 9.2 % tomato concentrate have the lowest apparent viscosity of 0.012 Pas and yield stress value of 0.0156 Pa as shown in Figure (28), which shows rheology properties as a function to the number of passages. At the first two passages, rheology measurements increase rapidly. After the second passage, the increasing continues with less intensity comparing to two first passages. This behavior is compatible with size measurements which showed that most of the size reduction is in the first two passages leading to the formation of a network of small fiber particles. However, between the 4th and 16th passages, the particles continue to break up less severity. Thus, the rheology properties increased slowly.

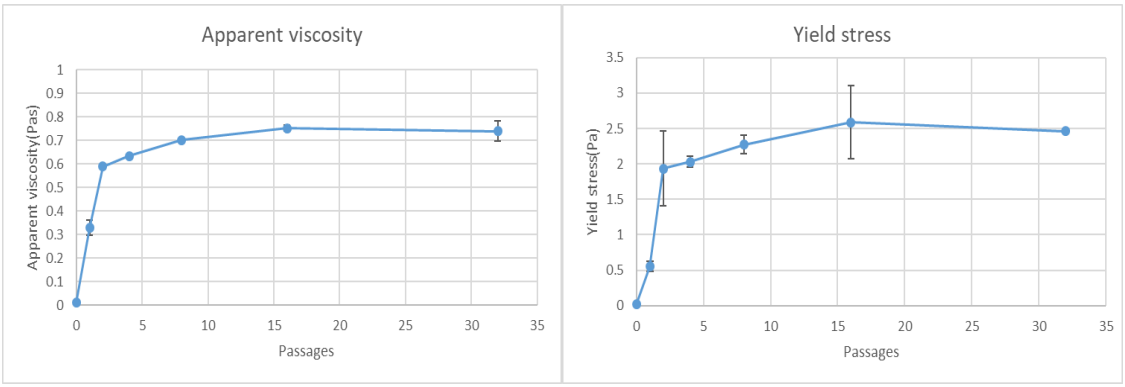

Figure 28: Apparent viscosity at shear rate of 10 s^{-1} and yield stress of 9.2% homogenized tomato juice as function of homogenization passages. The error bar represents 2± stander error.

After the 16th passage, it is possible to note small decrease in the apparent viscosity and yield stress. This occurs at the same time as the size of particles got smaller. This can be explained by that the size changing is very small after all these passages. Moreover, that it is possible that the repeated homogenization process could lead to destroying the fiber network instead of help to forming it.

5.5 Discussion on dominating break up mechanism

All the hypothetical mechanisms for fibre breakup (see Table 1), i.e. laminar shear, turbulent inertial and turbulent viscous, suggest that increasing of the homogenization pressure will increase fiber fragmentation leading to smaller fiber fragments. As seen in Section (3), the homogenized juice particles size is getting smaller with homogenization pressure. Qualitatively, this is in agreement with all the suggested mechanisms. However, the experimental results are shown that the slope value is -0.6 for 18,8% of tomato concentrate, and -0.5 for 9.2% tomato concentrate. These slope values do not match with the expected values for the different breaking mechanisms as shown in Table (1). Thus, none of the suggested mechanisms predict the scaling with homogenizing pressure seen in the results, suggesting that neither of them are dominating fiber break up in the high-pressure homogenizer.

For the influence of the continuous phase viscosity, experiment reveals that the most significant reduction in size occurs at lowest serum viscosity. Higher serum viscosity results in lower fragmentation efficiency. As shown in Figure (20), the obtained slope value is 0.22. These results are not in agreement with any of the hypothesis shown in Table (1). These propose that increasing serum viscosity lead to increased breakup effectivity and, hence, produce tomato suspension with smaller particles size. This prediction follows for both laminar viscous and turbulent viscous mechanisms. Furthermore, there is no match between the obtained results and the turbulent inertial regimes that assume no influence for the continuous phase viscosity on the fiber break up in the homogenization valve.

Moreover, the so-called squeezing theory is also not consistent with experimental observation. The results showed no major influence of the gap height on the particles break up and obtained particles were the same for all suggested gap height. These results do not fit with squeezing theory hypothesis of the obtained particles size should converge to gap height, thus smaller particles for smaller gap height. Also, the results from several passages can indicate no influence of the squeezing on the particles size breakup as the particles size went further smaller than the gap height value is (45 µm) see Figure (25).

6 Conclusion

Homogenization pressure proves to be the main factor that controlling fiber fragmentation in the homogenization valve and higher pressure means increasing the homogenization effectiveness, i.e. smaller particles size is achieved. The study shows that higher continuous phase viscosity led to smaller particles size for the homogenized juice. Tomato fiber shows the ability to continue to break up with each passage even after 32 passages and the point where there is no influence for the homogenization was not reached and further treated is needed. The investigation of the gap height influence has shown that no impact of the gap height on fiber break up in the high-pressure homogenizer.

This study has shown that improvement of rheology measurements of the unhomogenized juice with increasing the homogenization pressure and several passages homogenization by enhancing the interaction of fibers network.

The study rejected laminar shear, turbulent inertial and turbulent viscous as well as squeezing as the dominant breaking mechanisms. It is still unknown which mechanism (or combination thereof) that controls fiber breakup in high-pressure homogenizers.

7 Recommendations

Experimental works were performed using homogenizer that tested on milk products, which are different products comparing to tomato products, thus confirming the results using another homogenizer will be preferable.

Although there is a lot of literature study that does not consider or minimize the influence of the cavitation theory, cavitation could be a possible breaking mechanism. However, cavitation theory was not studied, due to machine limitation, especially in the second stage.

The study of each breaking mechanism individually conducted without considering that fragmentation could be the result of a combined work of different mechanisms. The research tried to explain the obtained results, but lack of information and literature studies concerning tomato fiber breakup in high-pressure homogenizer make it hard to reach for a suitable explanation, further investigation will be required.

More development method may be the key to provide more information and a more in-depth understanding of fiber fragmentation in the high-pressure homogenizer.

8 References

Augusto, P. E., Ibarz, A., & Cristianini, M. (2012). Effect of high pressure homogenization (HPH) on the rheological properties of a fruit juice serum model. *Journal of Food Engineering*, *111*(2), 474-477.

Augusto, P. E., Ibarz, A., & Cristianini, M. (2012). Effect of high pressure homogenization (HPH) on the rheological properties of tomato juice: Time-dependent and steady-state shear. *Journal of Food Engineering*, *111*(4), 570-579.

Bylund, G. (2015). *Dairy processing handbook*. Lund: Tetra Pak Processing Systems AB.

Bailey, R. (2018, March 16). Cell Wall Structure and Function. Retrieved from https://www.thoughtco.com/cell-wall-373613

Bayod, E. (2008). *Mircostructure and rheological properties of concentrated tomato suspensions during processing*.

Bengtsson, H., Hall, C., & Tornberg, E. V. A. (2011). Effect of physicochemical properties on the sensory perception of the texture of homogenized fruit and vegetable fiber suspensions. *Journal of texture studies*, *42*(4), 291-299.

CODEX, S. (2005). STAN 247-2005. *Codex Gen. Stand. Fruit Juices and Nectars. Rome: Food and Agriculture Organization*.

Chen, J., & Stokes, J. R. (2012). Rheology and tribology: Two distinctive regimes of food texture sensation. *Trends in Food Science & Technology*, *25*(1), 4-12.

Coccaro, Nicola, Giovanna Ferrari, and Francesco Donsì. "Understanding the break-up phenomena in an orifice-valve high pressure homogenizer using spherical bacterial cells (Lactococcus lactis) as a model disruption indicator." *Journal of Food Engineering* 236 (2018): 60-71.

Diels, A. M., Callewaert, L., Wuytack, E. Y., Masschalck, B., & Michiels, C. W. (2005). Inactivation of Escherichia coli by high-pressure homogenisation is influenced by fluid viscosity but not by water activity and product composition. *International Journal of Food Microbiology*, *101*(3), 281-291.

Engler, C. R., & Robinson, C. W. (1981). Disruption of Candida utilis cells in high pressure flow devices. Biotechnology and Bioengineering, 23(4), 765-780.

Elfick, J. (2018, November 10). Retrieved from http://www.uq.edu.au/_School_Science_Lessons/UNBiol1.html

Francis, F. J.,(Ed.). (1999). *Encyclopedia of food science and technology, 4-vol.set*. Wiley.

Fruit and vegetable processing - Ch011 Fruit and vegetable processing units - general approach; preliminary study; how to invest, install and operate a processing centre; modular units: From farm/family to community/business level (cont.). (n.d.). Retrieved from http://www.fao.org/docrep/V5030E/V5030E0w.htm

FAO (Food and Agriculture Organization of the United Nations). 2017. FAOSTAT Database. http://faostat3.fao.org/

Gaulin, A. (1904). *U.S. Patent No. 753,792*. Washington, DC: U.S. Patent and Trademark Office.

Gausman, H. W., Allen, W. A., & Escobar, D. E. (1974). Refractive index of plant cell walls. *Applied optics*, *13*(1), 109-111.

Goose, P. G., & Binsted, R. (1973). Tomato paste and other tomato products.

Goodwin, J. (2009). *Colloids and interfaces with surfactants and polymers*. John Wiley & Sons,196-199.

Håkansson, A. (2017). Scale-down failed–Dissimilarities between high-pressure homogenizers of different scales due to failed mechanistic matching. *Journal of Food Engineering*, *195*, 31-39.

Håkansson, A. (2015). Droplet breakup in high-pressure homogenizers. In *Engineering Aspects of Food Emulsification and Homogenization* (pp. 125-148). CRC Press Taylor & Francis Group Boca Raton, Fl.

Håkansson, A., Fuchs, L., Innings, F., Revstedt, J., Trägårdh, C., & Bergenståhl, B. (2011). High resolution experimental measurement of turbulent flow field in a high pressure homogenizer model and its implications on turbulent drop fragmentation. Chemical engineering science, 66(8), 1790-1801.

Hinze, J. O. (1955). Fundamentals of the hydrodynamic mechanism of splitting in dispersion processes. AIChE Journal, 1(3), 289-295.

Innings, F., & Trägårdh, C. (2007). Analysis of the flow field in a high-pressure homogenizer. *Experimental Thermal and Fluid Science*, *32*(2), 345-354.

Innings, F., Fuchs, L., & Trägårdh, C. (2011). Theoretical and experimental analyses of drop deformation and break-up in a scale model of a high-pressure homogenizer. *Journal of food engineering*, *103*(1), 21-28.

IDF, 2010. The world dairy situation 2010. *Bulletin of the International Dairy Federation* 446.

Innings, F. (2005). *Drop break-up in high-pressure homogenisers*. Food Engineering, Technology and Nutrition.

Innings, F., & Trägårdh, C. (2005). Visualization of the Drop Deformation and Break-Up Process in a High Pressure Homogenizer. *Chemical Engineering & Technology: Industrial Chemistry-Plant Equipment-Process Engineering-Biotechnology*, *28*(8), 882-891.

Innings, F., Fuchs, L., & Trägårdh, C. (2011). Theoretical and experimental analyses of drop deformation and break-up in a scale model of a high-pressure homogenizer. *Journal of food engineering*, *103*(1), 21-28.

Innings, F. (2015). High-pressure homogenizer design. *Engineering Aspects of Food Emulsification and Homogenization*, 149

Kubo, M. T. K., Augusto, P. E., & Cristianini, M. (2013). Effect of high pressure homogenization (HPH) on the physical stability of tomato juice. *Food research international*, *51*(1), 170-179.

Kertesz, Z. I. (1951). *Pectic substances*. Interscience Publishers, Inc.; New York.

Kolb, G., Wagner, G., & Ulrich, J. (2001). Untersuchungen zum Aufbruch von Einzeltropfen in Dispergiereinheiten zur Emulsionsherstellung. *Chemie Ingenieur Technik*, *73*(1-2), 80-83.

Kleinig, A. R., & Middelberg, A. P. (1998). On the mechanism of microbial cell disruption in high-pressure homogenisation. *Chemical Engineering Science*, *53*(5), 891-898.

Kleinig, A. R., & Middelberg, A. P. (1996). The correlation of cell disruption with homogenizer valve pressure gradient determined by computational fluid dynamics. Chemical Engineering Science, 51(23), 5103-5110.

Kolmogorov, A. (1949). On the breakage of drops in a turbulent flow. In Dokl. Akad. Navk. SSSR (Vol. 66, pp. 825-828).

Lopez-Sanchez, P., Svelander, C., Bialek, L., Schumm, S., & Langton, M. (2011). Rheology and Microstructure of Carrot and Tomato Emulsions as a Result of High-Pressure Homogenization Conditions. *Journal of Food Science*, *76*(1)

Lopez-Sanchez, P., Svelander, C., Bialek, L., Schumm, S., & Langton, M. (2011). Rheology and microstructure of carrot and tomato emulsions as a result of high-pressure homogenization conditions. *Journal of Food Science*, *76*(1), E130-E140.

Leonard, S. (1971). Tomato juice and tomato juice blends. *Tressler, DK Fruit and veg juice process technol*.

Lehkoživová, J., Karovičová, J., & Kohajdová, Z. (2009). The quality and authenticity markers of tomato ketchup. *Acta Chimica Slovaca*, *2*(2), 88-96.

Moore, E. K., Hoare, M., & Dunnill, P. (1990). Disruption of baker's yeast in a high-pressure homogenizer: New evidence on mechanism. *Enzyme and Microbial Technology*, *12*(10), 764-770.

Ouden, F. D., & Vliet, T. V. (1997). Particle size distribution in tomato concentrate and effects on rheological properties. *Journal of food science*, *62*(3), 565-567.

Phipps, L. W. (1975). The fragmentation of oil drops in emulsions by a high-pressure homogenizer. *Journal of Physics D: Applied Physics*, *8*(4), 448.

Phipps, L. W. (1974). Cavitation and separated flow in a simple homogenizing valve and their influence on the break-up of fat globules in milk. *Journal of Dairy Research*, *41*(1), 1-8.

Panalytical, M. (2018, August 25). Determining and Understanding the Yield Stress of Complex Fluids. Retrieved from https://www.azom.com/article.aspx?ArticleID=12448

Panozzo, A., Lemmens, L., Van Loey, A., Manzocco, L., Nicoli, M. C., & Hendrickx, M. (2013). Microstructure and bioaccessibility of different carotenoid species as affected by high pressure homogenisation: a case study on differently coloured tomatoes. *Food chemistry*, *141*(4), 4094-4100.

Rao, M. A. (2010). *Rheology of fluid and semisolid foods: principles and applications*. Springer Science & Business Media.

Rayner, M. (2015). Scales and Forces in Emulsification. *Engineering Aspects of Food Emulsification and Homogenisation*, 3-32.

Sriamornsak, P. (2003). Chemistry of pectin and its pharmaceutical uses: a review. *Silpakorn University International Journal*, *3*(1-2), 206-228.

Tornberg, E. (2016). Influence of fibers and particle size distribution on food rheology. In *Advances in Food Rheology and Its Applications* (pp. 177-208).

Trujillo, A. J., Roig-Sagués, A. X., Zamora, A., & Ferragut, V. (2016). High- Pressure Homogenization for Structure Modification. In *Innovative Food Processing Technologies* (pp. 315-344).

Thakur, B. R., Singh, R. K., & Nelson, P. E. (1996). Quality attributes of processed tomato products: a review. *Food Reviews International*, *12*(3), 375-401.

Thakur, B. R., Singh, R. K., Handa, A. K., & Rao, M. A. (1997). Chemistry and uses of pectin—a review. *Critical Reviews in Food Science & Nutrition*, *37*(1), 47-73.

Whittenberger, R. T., & Nutting, G. C. (1958). High viscosity of cell wall suspensions prepared from tomato juice. *Food Technology*, *12*(8), 420-424.

Walstra, P., & Smulders, P. E. (1998). Emulsion formation. *Modern aspects of emulsion science*, 56-99.

Walstra, P. (1993). Principles of emulsion formation. *Chemical Engineering Science*, *48*(2), 333-349.

Walstra, P., 1983. Formation of emulsions. In: *Encyclopedia of Emulsion Technology Volume I:Basic Theory*, Becher, P. (ed.), Marcel Dekker Inc., New York, 57–127.

9 Appendices

Appendix A: The correlation between d_{max} and ΔP for LV regime

The relation between the velocity gradient and gap velocity is given by equation (19):

$$G = \frac{\frac{1}{2}U_g}{h} \quad \text{(Eq.19)}$$

The gap height can obtain using equation (3) which can be rewritten as following:

$$h = \frac{Q}{2\pi r_e U_g} \quad \text{(Eq.20)}$$

U_g is function to homogenization pressure and can be obtained from Equation (5):

$${U_g}^2 = \frac{2\Delta p}{\rho_c} \quad \text{(Eq.21)}$$

By substituting Equations 20 and 21 in Equation (19), velocity gradient i.e. shear can experience by homogenization pressure:

$$G = \frac{2\pi r_e \Delta p}{\rho_c} \quad \text{(Eq.22)}$$

By substituting Equation (22) in Equation (9), maximum drop diameter can be expressed in terms of homogenization pressure:

$$d_{max} = \frac{\gamma We_{cr}\rho_c}{\pi r_e \eta_c \Delta p} \quad \text{(Eq.23)}$$

Base on Equation 23, It can be concluded that increasing homogenization pressure will lead to smaller particles size and expected slope will be $d_{max} \propto \Delta p^{-1}$.

Appendix B: The correlation between d_{max} and ΔP for TV and TI regimes

The rate of dissipation of turbulent kinetic energy can be estimated as function to homogenization pressure by substituting Equations (20) and (21) in Equation (11) as following:

$$\bar{\varepsilon} = \frac{\pi r_e \Delta p^2}{10 Q {\rho_c}^2} \quad \text{(Eq.24)}$$

For TI regime, the correlation between maximum drop size and homogenization pressure can be obtain by substituting Equation (24) in Equation (13):

$$d_{max} = \left(\frac{\pi r_e}{10 Q {\rho_c}^2}\right)^{-2/5} \Delta p^{-4/5} \gamma^{3/5} \rho_c^{-1/5} \quad \text{(Eq.25)}$$

Eq (25) shown that d_{max} is inversely proportional to $\Delta p^{4/5}$ and smaller particles size can be obtained.

For TV regime, maximum drop size can be calculated by substituting Equation (24) in Equation (15):

$$d_{max} = \left(\frac{\pi r_e}{10 Q {\rho_c}^2}\right)^{-1/2} \Delta p^{-1} \gamma \eta_c^{-1/2} \quad \text{(Eq.26)}$$

Thus, in TV regime keeping continuous phase viscosity constant and changing pressure will give smaller particles size and they are inversely proportional $d_{max} \propto \Delta p^{-1}$.

Appendix C: Effect of the pressure on particle size distribution and rheology measurements of tomato juice

Influence of pressure on the surface base mean diameter D_{32} and volume base mean diameter D_{43} for 18.8% tomato concentrate.

Pressure	D [3, 2] (µm)	D [3, 2] (µm)	Average (µm)	D [4, 3] (µm)	D [4, 3] (µm)	Average (µm)
0	144.063	146.661	145.362	299.497	306.65	303.0735
50	124.273	123.966	124.1195	285.225	282.031	283.628
100	93.509	94.123	93.816	247.291	248.015	248.015
200	47.91	38.232	43.071	163.086	154.537	163.086
300	28.891	21.38	25.1355	113.588	111.694	112.641
350	20.503	16.533	18.518	87.649	83.84	85.7445

Influence of pressure on the surface base mean diameter D_{32} and volume base mean diameter D_{43} for 9.2% tomato concentrate.

Pressure	D [3, 2] (µm)	D [3, 2] (µm)	Average (µm)	D [4, 3] (µm)	D [4, 3] (µm)	Average (µm)
0	146.042	141.688	143.865	303.451	300.758	302.1045
50	124.894	127.105	125.9995	285.253	290.511	287.882
100	88.778	90.094	89.436	243.426	246.952	248.015
200	34.259	31.975	33.117	171.777	178.299	163.086
300	17.845	16.882	17.3635	116.324	122.866	119.595
350	15.01	14.066	14.538	106.21	112.311	109.2605

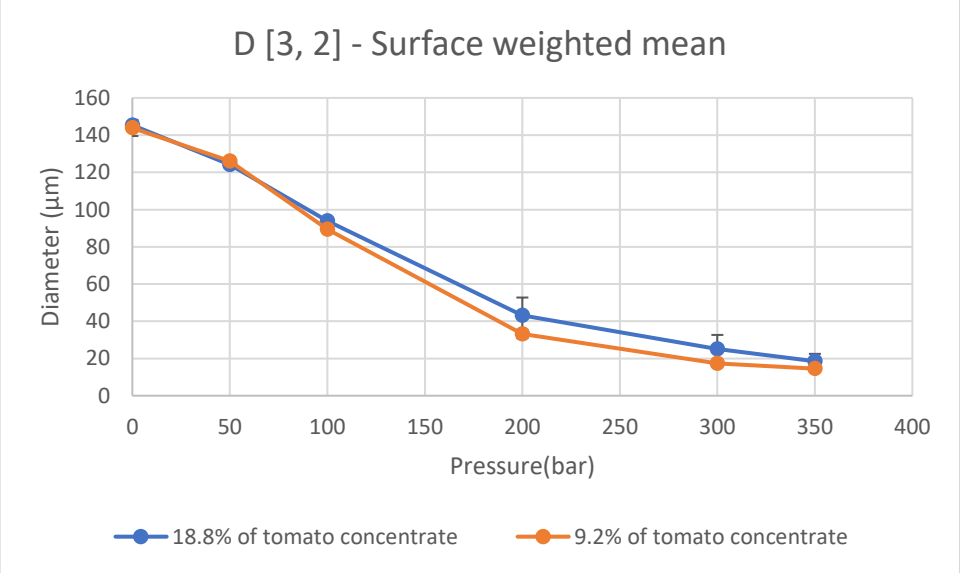

Surface base mean diameter D_{32} as function of homogenization pressure of 18.8% and 9.2% of tomato concentrate.

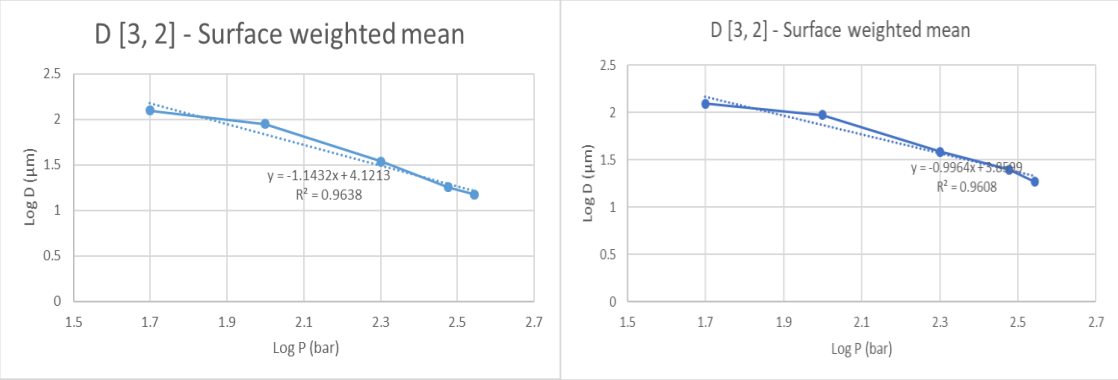

Log D_{32} as function of Log P of TJ (left)9.2% of tomato concentrate (right)18.8% of tomato concentrate.

95% confidence interval (the blue cells) of the slope of surface base mean diameter D_{32} and volume base mean diameter D_{43} as function of homogenization pressure for homogenized juice of 18.8% tomato concentrate.

D32						
SUMMARY OUTPUT						
Regression Statistics						
Multiple R	0,98					
R Square	0,961					
Adjusted R Squa	0,948					
Standard Error	0,082					
Observations	5					
ANOVA						
	df	*SS*	*MS*	*F*	*nificance F*	
Regression	1	0,493	0,493	73,577	0,0033	
Residual	3	0,02	0,007			
Total	4	0,513				
	Coefficien	*ndard E*	*t Stat*	*P-value*	*ower 95%*	*pper 95%*
Intercept	3,86	0,259	14,92	0,0007	3,0368	4,683
	-1	0,116	-8,58	0,0033	-1,366	-0,627

D43						
SUMMARY OUTPUT						
Regression Statistics						
Multiple R	0,957					
R Square	0,915					
Adjusted R Squa	0,887					
Standard Error	0,074					
Observations	5					
ANOVA						
	df	*SS*	*MS*	*F*	*nificance F*	
Regression	1	0,178	0,178	32,427	0,011	
Residual	3	0,016	0,005			
Total	4	0,195				
	Coefficien	*ndard E*	*t Stat*	*P-value*	*ower 95%*	*pper 95%*
Intercept	3,53	0,234	15,07	0,0006	2,784	4,275
X Variable 1	-0,599	0,105	-5,69	0,0107	-0,934	-0,264

95% confidence interval (the blue cells) of the slope of surface base mean diameter D_{32} and volume base mean diameter D_{43} as function of homogenization pressure for homogenized juice 9,2% of tomato concentrate.

D32

SUMMARY OUTPUT

Regression Statistics	
Multiple R	0,982
R Square	0,964
Adjusted R Squ	0,952
Standard Error	0,09
Observations	5

ANOVA

	df	*SS*	*MS*	*F*	*nificance F*
Regression	1	0,649	0,649	79,8217	0,003
Residual	3	0,024	0,008		
Total	4	0,673			

	Coefficien	*ndard E*	*t Stat*	*P-value*	*wer 95*	*pper 95%*
Intercept	4,121	0,285	14,47	0,00072	3,215	5,028
X Variable 1	-1,14	0,128	-8,934	0,00296	-1,55	-0,736

D43

SUMMARY OUTPUT

Regression Statistics	
Multiple R	0,971
R Square	0,943
Adjusted R Squa	0,924
Standard Error	0,052
Observations	5

ANOVA

	df	*SS*	*MS*	*F*	*nificance F*
Regression	1	0,136	0,136	49,899	0,0058
Residual	3	0,008	0,003		
Total	4	0,144			

	Coefficien	*ndard Er*	*t Stat*	*P-value*	*ower 95%*	*pper 95%*
Intercept	3,386	0,165	20,55	0,0003	2,8613	3,9098
X Variable 1	-0,523	0,074	-7,064	0,0058	-0,758	-0,287

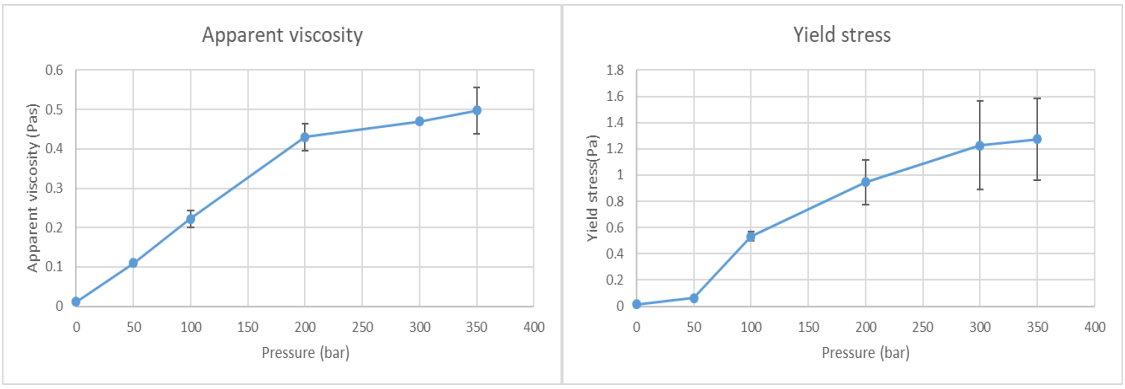

Apparent viscosity at shear rate of 10 s^{-1} and yield stress of 9.2%TJ as function of homogenization pressure of TJ of 9.2 of tomato concentrate.

Appendix D: Effect of serum viscosity on particles size of TJ

Effect of homogenization for several time on the surface base mean diameter D_{32} and volume base mean diameter D_{43}.

Serum viscosity (Pas)×10^{-3}	D [3, 2] (µm)	D [3, 2] (µm)	Average (µm)	D [4, 3] (µm)	D [4, 3] (µm)	Average (µm)
2.7	52.66	51.258	51.959	197.592	198.941	198.3
3.1	62.115	62.013	62.064	208.633	208.934	208.8
3.6	69.99	70.328	70.159	218.118	216.991	217.6
4.8	78.699	81.171	79.935	227.46	230.222	228.8
5.9	86.807	85.126	85.9665	237.99	236.254	237.1

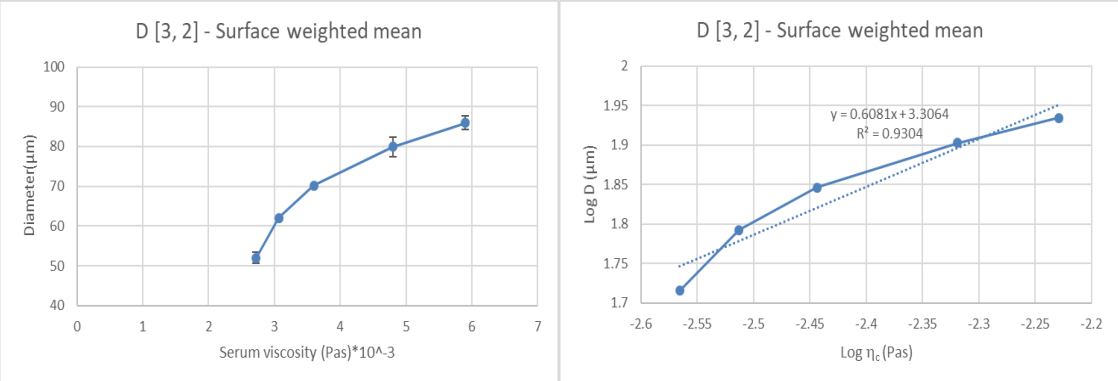

Influence of Serum viscosity of on the surface base mean diameter D_{32} of TJ juice.

95% confidence interval (the blue cells) of the slope of surface base mean diameter D_{32} and volume base mean diameter D_{43} as function of serum viscosity.

D_{32}						
SUMMARY OUTPUT						
egression Statistics						
Multiple R	0,965					
R Square	0,93					
Adjusted R	0,907					
Standard E	0,027					
Observatic	5					
ANOVA						
	df	*SS*	*MS*	*F*	*nificance F*	
Regressior	1	0,0284	0,028	40,076	0,008	
Residual	3	0,0021	7E-04			
Total	4	0,0305				
	Coefficien	*ndard Er*	*t Stat*	*P-value*	*wer 95%*	*pper 95%*
Intercept	3,306	0,2322	14,24	0,0008	2,567	4,045
X Variable	0,608	0,0961	6,331	0,008	0,302	0,914

D_{43}						
SUMMARY OUTPUT						
Regression Statistics						
Multiple R	0,984					
R Square	0,969					
Adjusted R	0,959					
Standard E	0,006					
Observatic	5					
ANOVA						
	df	*SS*	*MS*	*F*	*nificance F*	
Regressior	1	0,004	0,004	94,13	0,002	
Residual	3	1E-04	4E-05			
Total	4	0,004				
	Coefficien	*ndard E*	*t Stat*	*P-value*	*wer 95%*	*pper 95%*
Intercept	2,868	0,055	52,4	2E-05	2,694	3,042
X Variable	0,22	0,023	9,702	0,0023	0,148	0,292

Appendix E: Effect of several passages on particle size distribution of tomato juice.

Effect of homogenization for several time on the surface base mean diameter D_{32} and volume base mean diameter D_{43} of 9.2% of tomato concentrate.

NH	D [3, 2] (µm)	D [3, 2] (µm)	Average (µm)	D [4, 3] (µm)	D [4, 3] (µm)	Average (µm)
0	146.042	141.688	143.865	299.497	306.65	303.0735
1	64.141	60.753	62.447	216.137	213.093	214.615
2	13.04	12.158	12.599	117.965	111.208	114.5865
4	8.871	8.769	8.82	90.069	87.62	88.8445
8	5.545	5.339	5.442	46.965	46.755	46.86
16	4.462	4.306	4.384	29.361	30.172	29.7665
32	3.701	3.447	3.574	21.784	21.292	21.538

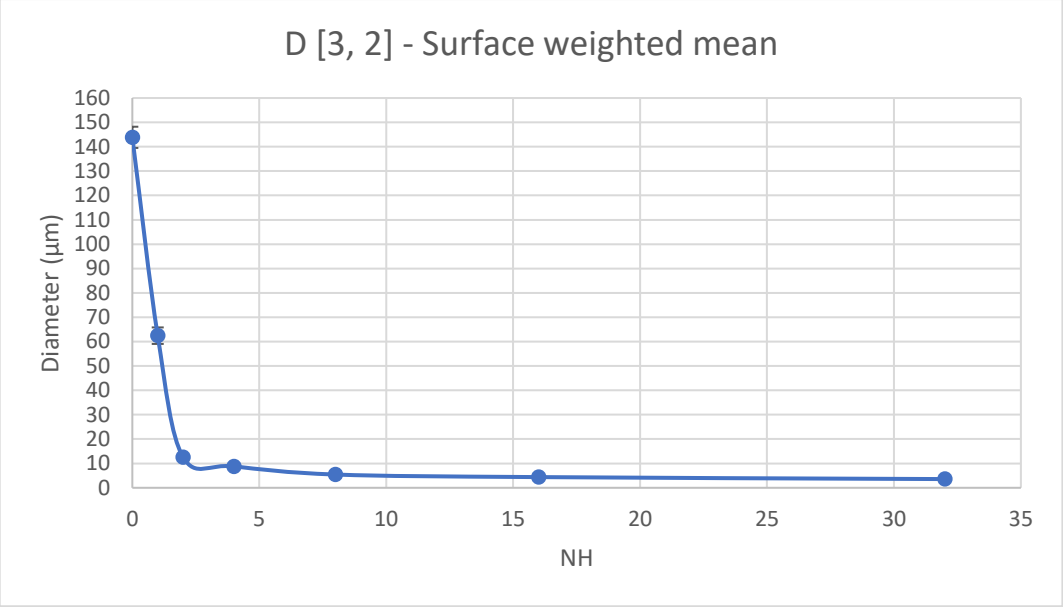

Influence of homogenization for several time on the surface base mean diameter D_{32} of 9.2% of tomato concentrate.

Appendix F: Gap height calculation

The values of gap height were obtained using Phipps equation (equation (4), Phipps, 1975) in MATLAB. Phipps equation was used by solving for h. The geometrical parameters of homogenizer are shown in the Table (2) and flow rate values are 304, 219 and 161 L/h. The homogenization pressure is set to 150 bar first stage homogenization pressure and 20 bars for the second stage. The density and kinetic viscosity of continuous phase assumed to be 1005g/cm^3 and 8.9 m^2/s respectively at the room temperature.

Phipps equation contains three terms which are Δp_{IC} , Δp_{gap} and Δp_{OC}. Δp_{IC} and Δp_{OC} was found directly from equation (4). Δp_{gap} was calculated as following:

$$\Delta p_{gap} = \frac{6\rho_c \eta_c Q}{\pi h^3} ln \frac{r_e}{r_i} \qquad \text{Re}_i < 500 \text{ (Eq.26)}$$

Or by using:

$$\Delta p_{gap} = \frac{5\rho_c \eta_c^{3/5}}{h^3} \left[\frac{Q}{2\pi}\right]^{7/5} \left[\frac{1}{r_i^{2/5}} - \frac{1}{r_e^{2/5}}\right] + \frac{1}{2} \qquad \text{Re}_i > 500 \text{ (Eq.27)}$$

And Re_i was found by using equation (28):

$$Re_i = Re\frac{r_e}{r_i} \quad \text{(Eq.28)}$$

Re was calculated from equation (2).

After found Δp_{IC} , Δp_{gap} and Δp_{OC} as function for h, it is possible to solve the equation and found the value of h. The obtained gap height is shown in the following table:

Summary of calculated gap height.

First stage pressure (bar)	Second stage pressure (bar)	Flow rate (L/h)	Stroke time (s)	gap-height (µm)	Gap-velocity (m/s)
150	20	304	0.45	45	198
150	20	219	0.625	34	190
150	20	161	0.85	26	181

Appendix G: Effect of the gap height on the particle's diameter of homogenized TJ with One-way ANOVA analysis.

Influence of homogenization with different gap height on the volume base mean diameter D_{43} of18.8%TJ.

Gap-height (µm)	D [4, 3] (µm)	D [4, 3] (µm)	D [4, 3] (µm)	D [4, 3] (µm)	Average (µm)
45	219.259	217.185	220.665	219.081	219.0475
34	217.905	212.585	228.693	227.075	221.5645
26	222.381	221.335	230.83	228.714	225.815

One-way ANOVA analysis of D_{43} of 18.8% homogenized TJ.

ANOVA - D_{43}

Source of Variation	*SS*	*df*	*MS*	*F*	*P-value*	*F crit*
Between Groups	93.60146	2	46.80073033	1.706999	0.235228	4.256495
Within Groups	246.7527	9	27.41697022			
Total	340.3542	11				

Influence of homogenization with different gap height on the surface base mean diameter D_{32} of 18.8%TJ.

Gap-height (µm)	D [3, 2] (µm)	D [3, 2] (µm)	D [3, 2] (µm)	D [3, 2] (µm)	Average (µm)
45	74.587	70.912	71.193	71.006	71.9245
34	72.373	65.808	79.002	77.916	73.77475
26	72.865	73.207	81.202	79.638	76.728

One-way ANOVA analysis of D_{32} of 18.8% homogenized TJ.

ANOVA-D_{32}

Source of Variation	*SS*	*df*	*MS*	*F*	*P-value*	*F crit*
Between Groups	46.9583	2	23.47914858	1.20608	0.343507	4.256495
Within Groups	175.2059	9	19.46732064			
Total	222.1642	11				

Influence of homogenization with different gap height on the volume base mean diameter D_{43} of 9.2%TJ.

Gap-height (µm)	D [4, 3] (µm)	D [4, 3] (µm)	D [4, 3] (µm)	D [4, 3] (µm)	Average (µm)
45	212.712	207.845	216.137	213.093	212.4468
34	204.53	203.963	212.988	215.12	209.1503
26	210.422	209.852	212.563	216.951	212.447

One-way ANOVA analysis of D_{43} of 9.2% homogenized TJ.

ANOVA-D_{43}

Source of Variation	*SS*	*df*	*MS*	*F*	*P-value*	*F crit*
Between Groups	28.98063	2	14.49032	0.790205	0.48287	4.256495
Within Groups	165.0367	9	18.33741			
Total	194.0173	11				

Influence of homogenization with different gap height on the surface base mean diameter D_{32} of 9.2%TJ.

Gap-height (µm)	D [3, 2] (µm)	D [3, 2] (µm)	D [3, 2] (µm)	D [3, 2] (µm)	Average (µm)
45	65.898	60.313	64.141	60.753	62.77625
34	56.082	55.639	62.435	63.732	59.472
26	60.155	59.821	60.529	67.281	61.9465

One-way ANOVA analysis of D_{32} of 9.2% homogenized TJ.

ANOVA-D_{32}

Source of Variation	*SS*	*df*	*MS*	*F*	*P-value*	*F crit*
Between Groups	23.6396	2	11.8198	0.940789	0.425577	4.256495
Within Groups	113.0734	9	12.56371			
Total	136.713	11				

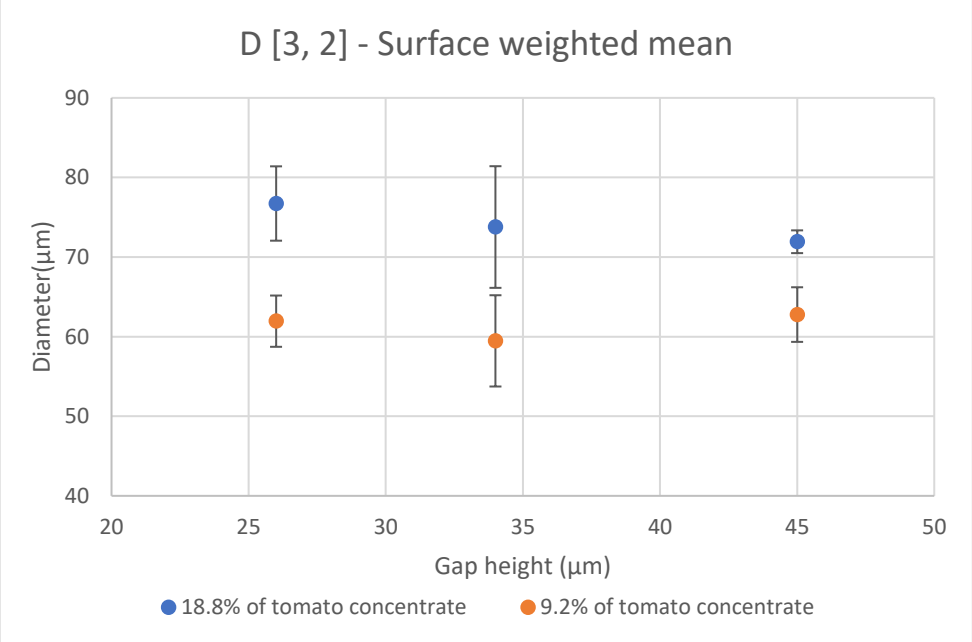

Influence of homogenization with different gap height on the surface base mean diameter D_{32} of 9.2%TJ and 18.8%TJ.

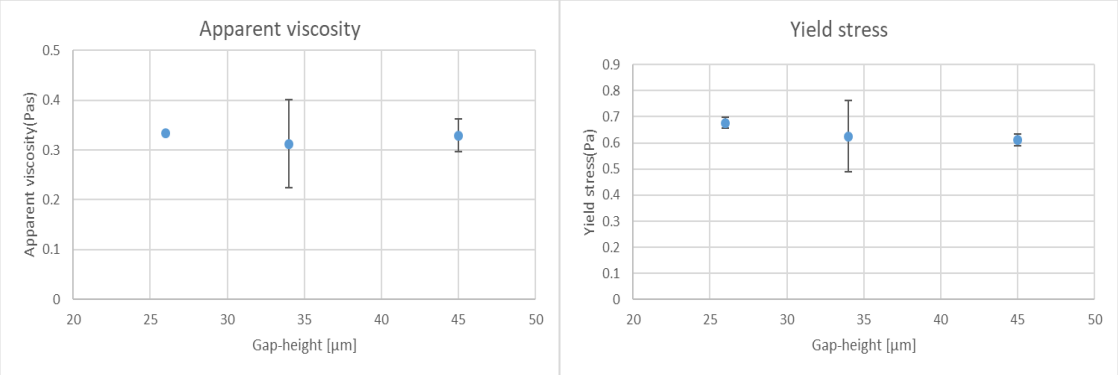

Apparent viscosity at shear rate of 10 s^{-1} and yield stress at different gap height for 9.2% of tomato juice.

Appendix H: Specification of raw material

SPECIFICATIONS
TOMATO PASTE 28/30% WARM-BREAK

Code: 209 220 L ASEPTIC BAGS	DATE: 10/07/2014 PAGE: 1 of 4

1. GENERAL DESCRIPTION

The product is the result of the concentration of fresh tomato pulp, after removal of skins and seeds and refinement by screening. The raw fruit material is clean, freshly harvested and full red-ripe fruit of the species *Lycopersicum esculentum P. Miller*. Screen size 1,0 – 1,2mm.

The tomato paste is produced by a sound industrial warm break process to yield commercially sterile product which contains no chemical preservatives or other additives of any kind.

The process is carried out in good sanitary conditions using sound manufacturing techniques and the Company has implemented the HACCP System.

2. SENSORY CHARACTERISTICS

Appearance	- uniform intense red
Texture	- homogeneous, without seeds, skins and other foreign matter
Taste	- bland, pleasant taste of ripe tomatoes, without any burned, bitter or any other off taste or foreign taste

3. CHEMICAL CHARACTERISTICS

Parameter	**Value**
Concentration	28/30%
pH	< 4.50
Howard Mould Count	< 70%
Total Acidity	< 10% of dry weight
Volatile Acidity	< 0.4% of dry weight
Sugars	> 42% of dry weight
Mineral Impurities	< 0.1% of dry weight
Black Specks	

Identification	Diameter	Maximum Admitted
Large Black points	> 1,0 mm	0
Medium Black points	0.5 – 1.0 mm	4
Small Black points	< 0.5 mm	16
Total of points		20

SPECIFICATIONS
TOMATO PASTE 28/30% WARM-BREAK

Code: 209 220 L ASEPTIC BAGS	DATE: 10/07/2014
	PAGE: 2 of 4

Parameter	**Value**	
Copper	< 20	mg/Kg
Lead	< 1.5	mg/Kg
Arsenic	< 1.0	mg/Kg
Tin	< 100	mg/Kg
Zinc	< 50	mg/Kg
Cadmium	< 0.03	mg/Kg
Mercury	< 0.005	mg/Kg

4. PHYSICAL CHARACTERISTICS

Parameter	**Value**
Bostwick	4,0 - 7,0 cm (12.5°Brix, 30sec. at 20°C)
Colour a/b (Gardner)	> 2.05 (BCR Tile)
L value (Gardner)	> 22.8

5. MICROBIOLOGICAL CHARACTERISTICS

Parameter	**Value**	**Analysis Method**
TVC	< 1000 colony in 1g	ISO 4833
Yeasts	< 10 colony in 1g	NP 3277-1
Moulds	< 10 colony in 1g	NP 3277-1
Lactobacillus	< 10 colony in 1g	MRS + Talium Acetat + Trifenil Tetrazolio (red colony counting)
Coliforms	< 10 colony in 1g	NP 2164
Eschericia coli	Negative in 1g	NP 2308
Thermophilic Aerobic Bacteria Spores	< 150 colony in 10g	KRAFT USA
Flat Sour Bacteria Spores	< 75 colony in 10g	KRAFT USA
Termophilic Anaerobic Bacteria Spores (6 tubes)	4 max.	KRAFT USA
Bacillus cereus	Variable, in general <100 colony in 1g	ISO 7932

6. NUTRITIONAL VALUES/100g

Parameter	**Value**
Energy	83 Kcal / 355 KJ
Protein	4.2 g
Carbohydrate	16.2 g
Total Fat	0.2 g
Fibre	6.3 g